TABLE 1 Clinical and biochemical characteristics of patients with HCV infection

Characteristic	CH (n = 28)	LC (n = 17)	LC + HCC (n = 32)
Males (%)	12 (43)	4 (24)	19 (59)
Age	58.6 ± 11.2	65.8 ± 11.0	66.3 ± 7.3
ALP (normal range 98–251 U/l)	258 ± 65.3	404.4 ± 183.9	386.2 ± 117.7
AST (normal range 12–31 U/l)	66.1 ± 49.4	84.8 ± 28.0	86.4 ± 46.9
ALT (normal range 12–35 U/l)	90.3 ± 76.2	75.8 ± 38.2	73.8 ± 36.4
Bilirubin (mg/dl)	0.7 ± 0.2	1.5 ± 1.1	1.1 ± 0.7
Albumin (g/dl)	4.3 ± 1.0	3.6 ± 0.6	3.5 ± 0.5
Prothrombin time (%)	101.6 ± 18.2	73.6 ± 17.3	83.3 ± 20.3
Cholinesterase (normal range 160–400 IU/l)	257.4 ± 74.4	150.0 ± 59.0	141.9 ± 70.7
Total cholesterol (mg/dl)	174.0 ± 36.0	165.9 ± 36.9	142.2 ± 30.0
Platelets ($10^3/\mu l$)	187 ± 65	105 ± 37	91 ± 38
Fibrosis stage	F0:1/F1:14/F2:6/F3:3 (n = 24)	F4:9 (n = 9)	F3:1/F4:5 (n = 6)
HCV serotype	1:17/2:7 (n = 24)	1:10/2:2 (n = 12)	1:2/2:2 (n = 4)

ALP, alkaline phosphatase; AST, aspartate aminotransferase; ALT, alanine aminotransferase. Values expressed are means ± SD.

ligand-binding protein (IL-6R, gp80) and a signal transduction protein (gp130) [12]. When IL-6 binds to a cell through IL-6R (gp80), the complex facilitates its interaction with a second IL-6 receptor molecule, gp130, thereby triggering intracellular signal transduction [13]. In addition to their roles as membrane-bound proteins, IL-6R and gp130 also occur as receptors shed into the serum [14]. In several conditions, such as myeloma, chronic arthritis, and autoimmune diseases, elevated levels of soluble IL-6R (sIL-6R) have been observed [15]. sIL-6R and soluble gp130 (sgp130) have different functions. sIL-6R bound to IL-6 can interact with membrane-bound gp130 and thereby trigger activation of intracellular signaling pathways [16]. This can lead to an enhanced IL-6-mediated response.

The shed signal transducer, sgp130, itself can bind the IL-6/sIL-6R complex [17]. The resulting trimeric complex is no longer able to interact with membrane-bound gp130. In this case, sgp130 acts as an antagonist. Therefore, the biological activity of IL-6 depends on the balance of sIL-6R and sgp130. Previous studies have concentrated only on the behavior of IL-6 circulating levels in various liver diseases [18]. In this study, we evaluated serum levels of IL-6 and soluble forms of IL-6 receptors (sIL-6R, sgp130) in patients with hepatitis C virus (HCV) infections.

MATERIALS AND METHODS

Patients

We studied 77 patients with various degrees of chronic liver disease (CLD) related to HCV infection (Table 1). Of the patients, 28 had chronic hepatitis, 17 liver cirrhosis, and 32 had liver cirrhosis plus hepatocellular carcinoma (HCC). The diagnosis of HCC was made by several imaging modalities and confirmed histologically by sonography-guided fine-needle biopsy specimens in all patients. At the time of the study, none of the patients was receiving or had previously received interferon therapy. All patients were positive for anti-HCV antibodies detected by a third-generation enzyme immunoassay containing HCV antigens from the viral core and from areas of the nonstructural NS3, NS4, and NS5 regions (Ortho HCV SAVe 3.0; Ortho, Raritan, NJ) and were positive for HCV RNA in the serum as assessed by means of nested reverse transcription polymerase chain reaction. Viral serotyping was performed on 40 patients. Liver biopsy was performed on 39 patients; the degree of liver fibrosis was assessed using the METAVIR system [19]. All patients enrolled in this study were regularly followed with liver function tests every month and with ultrasonography or computed tomography of liver every 4 months. Of these, patients with marked fluctuations in these tests were excluded from this study. Patients with other concomitant causes of liver disease, such as autoimmunity or alcohol abuse (more than 40 g alcohol daily intake), or patients with metabolic disease, infections, or renal dysfunctions were not included in the study to avoid possible confounding factors. All patients were negative for hepatitis B surface antigen and had no symptom or sign related to HIV, cytomegalovirus, and *Toxoplasma gondii* infection.

None of the patients suffered from hemolytic anemia or renal failure or manifested features compatible with the presence of disseminated intravascular coagulation. In addition, sera from 23 healthy volunteers were used as controls (10 males and 13 females, mean age 45.5 ± 13.2 years). All healthy volunteers presented as normal in liver function tests, with negative serology for viral hepatitis and no history of liver disease.

Enzyme-Linked Immunosorbent Assay

For duplicate measurements solid-phase Quantikine Immunoassays (R&D Systems, Minneapolis, MN, USA)

were used to measure serum IL-6, sIL-6R, and sgp-130 according to the manufacturer's instructions.

Statistical Analysis

Data are presented as the means ± SD. The differences between quantitative variables were evaluated with the Mann–Whitney U test. A p value <0.05 for two-sided tests was considered statistically significant. The correlation between two variables was analyzed using the Spearman rank correlation test. Statistical analysis was performed with StatView software (SAS Institute, Inc., Cary, NC, USA). A p value <0.05 was required for statistical significance.

RESULTS

A total of 77 patients were studied. Of these, 35 were male and 42 female, with a mean age of 63.4 ± 10.3 years. According to the disease progression, the patients were divided into three groups (chronic hepatitis, liver cirrhosis, and liver cirrhosis plus HCC). The main clinical, biochemical, and functional characteristics of the patients are presented in Table 1.

Serum levels of IL-6 were measured in patients with HCV infections and were significantly higher in these patients than in healthy subject (Figure 1). Furthermore, this analysis revealed that circulating IL-6 levels were significantly higher in patients with liver cirrhosis (LC) than in patients with chronic hepatitis (CH).

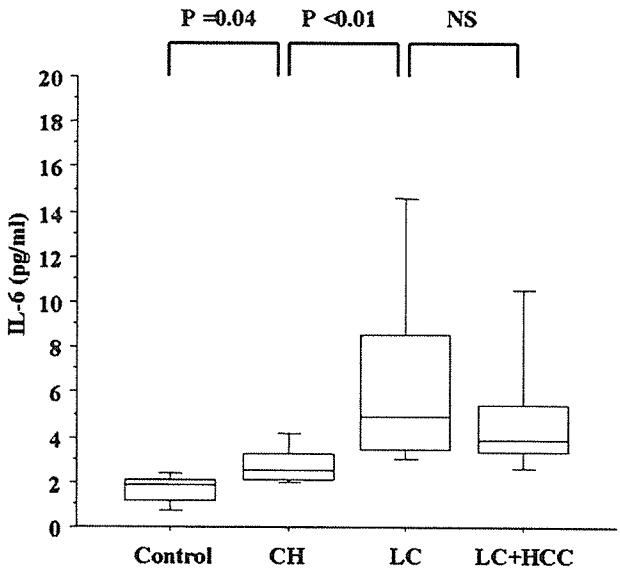

FIGURE 1 Serum IL-6 levels in patients with HCV infection and healthy controls. CH, chronic hepatitis; LC, liver cirrhosis; LC+HCC, liver cirrhosis plus hepatocellular carcinoma. The box contains the values between the 25th and the 75th percentiles and the horizontal line is the median. The error bars stretch to the 10th and the 90th percentiles.

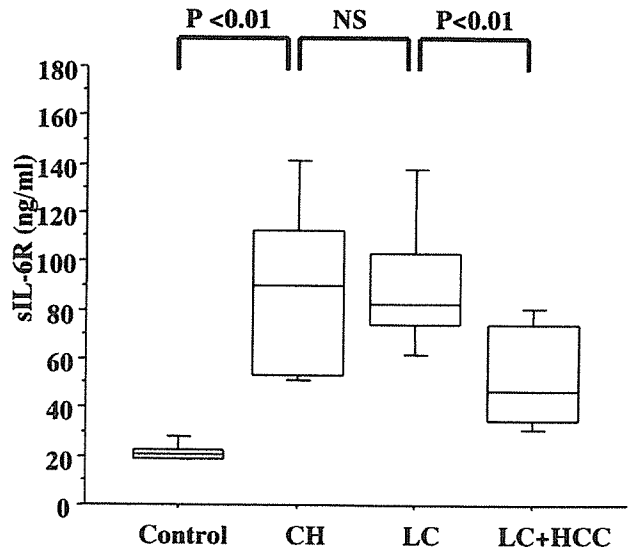

FIGURE 2 Serum sIL-6R levels in patients with HCV infection and healthy controls.

As presented in Figure 2, serum sIL-6R levels of patients with HCV infection were significantly higher than those in healthy subjects. No difference in sIL-6R level was detected between patients with CH and LC. However, sIL-6R levels varied significantly among patients with LC. That is, LC patients with HCC exhibited significantly lower levels of sIL-6R than did LC patients without HCC.

Serum levels of sgp130, which inhibits the action of IL-6, were also measured in patients with HCV infection (Figure 3). Patients with LC either with or without HCC exhibited elevated sgp130 values compared with healthy subjects. Conversely, no significant difference was observed in serum sgp130 levels between healthy subjects and patients with chronic hepatitis.

The relationships among IL-6, sIL-6R, sgp130, and clinicobiochemical parameters were also investigated. As presented in Figure 4, total bilirubin was significantly correlated with circulating sgp130 ($r = 0.49$, $p = 0.001$). In contrast, cholinesterase ($r = -0.48$, $p = 0.002$) and prothrombin time ($r = -0.39$, $p = 0.014$) were significantly inversely correlated with circulating sgp130 (Figure 5). Thus, we observed that in patients with HCV-related CLD, elevated levels of sgp130 were associated with impaired liver functions.

DISCUSSION

IL-6 plays a significant role in liver regeneration in conjunction with additional growth factors such as HGF or TNF-α [20,21]. Previous reports have demonstrated elevated IL-6 levels in patients with acute and chronic

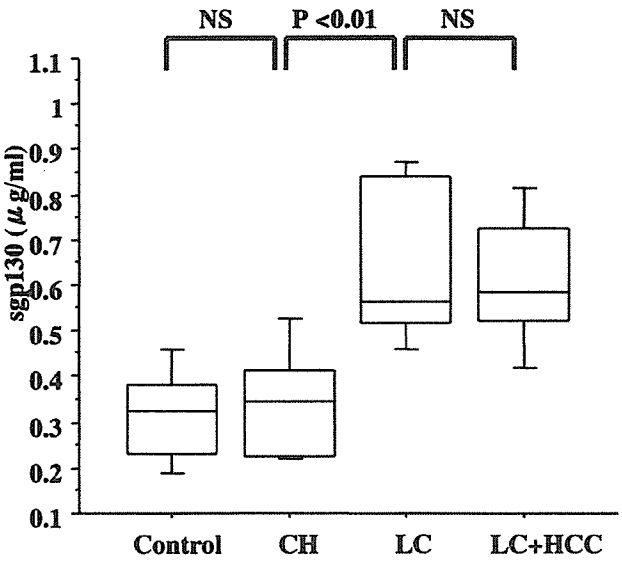

FIGURE 3 Serum sgp130 levels in patients with HCV infection and healthy controls.

liver disease [10,11,18]. The elevated levels of serum IL-6 were also demonstrated in HCV-infected patients [22,23]. However, it is unknown whether this cytokine activation represents only an epiphenomenon. To clarify the role of IL-6 in chronic liver disease, we studied the levels of soluble IL-6 receptors, which affect the biological effects of IL-6 in addition to IL-6 itself. The circulating levels of IL-6 and its soluble receptors have been demonstrated to be modulated by various diseases [24,25]. We therefore measured this cytokine and its soluble receptors in HCV-infected patients without any associated diseases or complications, such as infection, inflammation, or renal dysfunction.

One of the principle findings of this study was that both IL-6 and sIL-6R proteins were elevated in patients with HCV infection. In addition, the levels of IL-6 were significantly higher in patients with LC than in those with CH. Our data are consistent with those of a previous study demonstrating elevated circulating levels of sIL-6R in patients with liver cirrhosis [26].

sIL-6R is a ligand-binding protein that constitutes the extracellular part of the IL-6 receptor. sIL-6R markedly prolongs the IL-6 plasma half-life, and sIL-6R-bound IL-6 can interact with membrane-bound gp130 and thereby lead to activation of the intracellular signaling pathway [27]. This can lead to an enhanced IL-6-mediated response. Additionally, through this mechanism, primary unresponsive cells expressing only gp130 and no gp80 can be activated through the sIL-6R/IL-6 complex. This process has been called "*trans*-signaling" [28]. Considering this enhancing role of sIL-6R, we speculate that high levels of sIL-6R might potentiate the effects of IL-6 in HCV-induced chronic hepatitis or liver cirrhosis.

Results from studies using IL-6 knockout mice have indicated that IL-6 might be involved in hepatocyte proliferation [29]. These observations may suggest that the IL-6/sIL-6R system could be involved in liver regeneration after liver injury. Although the pathophysiological role of elevated IL-6/sIL-6R in HCV infection was not elucidated in this study, it could consist of a regenerative response against liver damage or inflammation.

Additional evidence supporting the idea that IL-6 plays a role in hepatocyte proliferation has come from experiments using double-transgenic mice expressing IL-6 and sIL-6R [30,31]. In these mice, hepatocyte proliferation was evident in the periportal area, and hyperplastic nodules were also observed. It is possible that elevated levels of IL-6/sIL-6R contribute to nodular regenerative changes in patients with HCV-induced liver cirrhosis. However, IL-6/sIL-6R may not be involved in the HCC association, because sIL-6R levels of LC patients with HCC were significantly lower than those without HCC.

Another main finding is that sgp130 levels were significantly higher in LC patients than in patients with chronic hepatitis. We evaluated the relationship between sgp130 levels and liver function tests, such as total bilirubin, cholinesterase, and prothrombin time. We observed that the increase in sgp130 is linked to impaired liver functions, including elevated bilirubin levels, prolonged prothrombin time, and reduced serum cholinesterase levels. Therefore, these findings may suggest that sgp130 elevation is related to progression of liver dysfunction as well as hepatic decompensation in patients with HCV-related CLD.

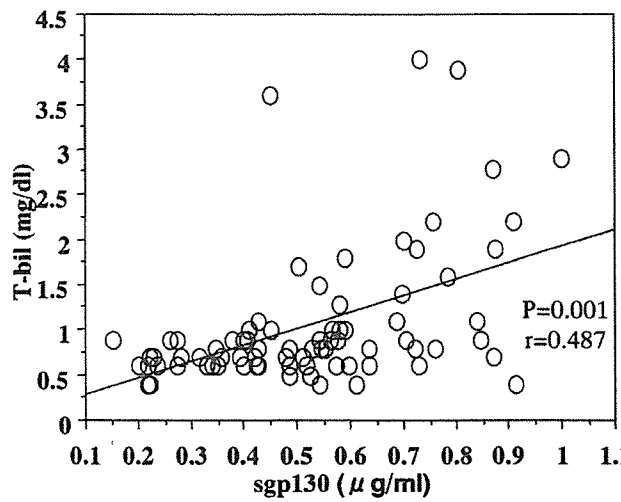

FIGURE 4 Correlation between individual values of total bilirubin and sgp130 in patients with HCV infection. T-bil, total bilirubin.

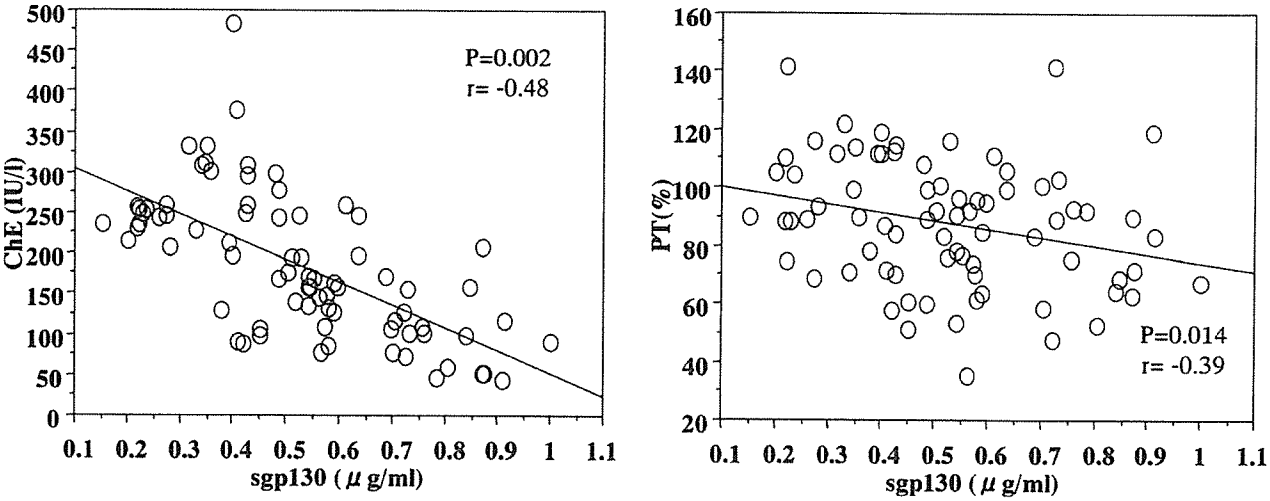

FIGURE 5 (A) Correlation between individual values of cholinesterase and sgp130 in patients with HCV infection. ChE, cholinesterase. (B) Correlation between individual values of prothrombin time and sgp130 in patients with HCV infection. PT, prothrombin time.

sIL-6R and sgp130 have different functions. The shed signal transducer sgp130 can itself bind the IL-6/sIL-6R complex and inhibit the action of IL-6. After injury, the liver has a remarkable capacity to restore major tissue loss through regeneration. IL-6 is an essential cytokine involved in liver regeneration. In fact, our data demonstrated that IL-6 and sIL-6R were significantly elevated in patients with chronic hepatitis and LC. However, under clinical conditions under which circulatory sgp130 is elevated, the IL-6/sIL-6R system may not maintain the liver regeneration. Although the exact mechanism by which sgp130 is elevated in LC patients was not elucidated in this study, this aberrant induction of sgp130 may lead to the abrogated IL-6/sIL-6R biological function and the development of liver dysfunctions and subsequent hepatic insufficiency in LC patients. Elevated levels of IL-6 and sIL-6R in HCV-related CLD likely contribute to compensatory hepatocyte growth during chronic liver injury. However, sgp130 levels in LC patients might antagonize the IL-6-mediated hepatotropic effect within the liver and could contribute to the impaired liver regeneration.

In conclusion, in this study, we have demonstrated that a progressive decline in liver function in patients with HCV-related CLD was paralleled by an increase in circulating sgp130 levels.

REFERENCES

1. Hirano T, Akira S, Taga T, Kishimoto T: Biological and clinical aspects of interleukin 6. Immunol Today 11:443, 1990.
2. Akira S, Taga T, Kishimoto T: Interleukin-6 in biology and medicine. Adv Immunol 54:1, 1993.
3. Barton BE: IL-6: insights into novel biological activities. Clin Immunol Immunopathol 85:16, 1997.
4. Heinrich PC, Castell JV, Andus T: Interleukin-6 and the acute phase response. Biochem J 265: 621, 1990.
5. Akira S, Kishimoto T: IL-6 and NF-IL6 in acute-phase response and viral infection. Immunol Rev 127:25, 1992.
6. Michalopoulos GK, DeFrances MC: Liver regeneration. Science 276:60, 1997.
7. Streetz KL, Luedde T, Manns MP, Trautwein C: Interleukin 6 and liver regeneration. Gut 47:309, 2000.
8. Blindenbacher A, Wang X, Langer I, Savino R, Terracciano L, Heim MH: Interleukin 6 is important for survival after partial hepatectomy in mice. Hepatology 38:674, 2003.
9. Galun E, Axelrod JH: The role of cytokines in liver failure and regeneration: potential new molecular therapies. Biochim Biophys Acta 1592:345, 2002.
10. Genesca J, Gonzalez A, Segura R, Catalan R, Marti R, Varela E, Cadelina G, Martinez M, Lopez-Talavera JC, Esteban R, Groszmann RJ, Guardia J: Interleukin-6, nitric oxide, and the clinical and hemodynamic alterations of patients with liver cirrhosis. Am J Gastroenterol 94: 169, 1999.
11. Kakumu S, Shinagawa T, Ishikawa T, Yoshioka K, Wakita T, Ito Y, Takayanagi M, Ida N: Serum interleukin 6 levels in patients with chronic hepatitis B. Am J Gastroenterol 86:1804, 1991.
12. Taga T, Kishimoto T: Gp130 and the interleukin-6 family of cytokines. Annu Rev Immunol 15:797, 1997.

13. Jones SA, Rose-John S: The role of soluble receptors in cytokine biology: the agonistic properties of the sIL-6R/IL-6 complex. Biochim Biophys Acta 1592:251, 2002.
14. Heinrich PC, Graeve L, Rose-John S, Schneider-Mergener J, Dittrich E, Erren A, Gerhartz C, Hemann U, Lutticken C, Wegenka U: Membrane-bound and soluble interleukin-6 receptor: studies on structure, regulation of expression, and signal transduction. Ann N Y Acad Sci 762:222, 1995.
15. Jones SA, Horiuchi S, Topley N, Yamamoto N, Fuller GM: The soluble interleukin 6 receptor: mechanisms of production and implications in disease. FASEB J 15:43, 2001.
16. Kallen KJ: The role of transsignalling via the agonistic soluble IL-6 receptor in human diseases. Biochim Biophys Acta 1592:323, 2002.
17. Jostock T, Mullberg J, Ozbek S, Atreya R, Blinn G, Voltz N, Fischer M, Neurath MF, Rose-John S: Soluble gp130 is the natural inhibitor of soluble interleukin-6 receptor transsignaling responses. Eur J Biochem 268:160, 2001.
18. Rehermann B, Trautwein C, Boker KH, Manns MP: Interleukin-6 in liver diseases. J Hepatol 15:277, 1992.
19. Bedossa P, Poynard T: An algorithm for the grading of activity in chronic hepatitis C. The METAVIR Cooperative Study Group. Hepatology 24:289, 1996.
20. Yamada Y, Kirillova I, Peschon JJ, Fausto N: Initiation of liver growth by tumor necrosis factor: deficient liver regeneration in mice lacking type I tumor necrosis factor receptor. Proc Natl Acad Sci USA 94:1441, 1997.
21. Fausto N: Liver regeneration. J Hepatol 32(1 Suppl):19, 2000.
22. Lapinski TW: The levels of IL-1beta, IL-4 and IL-6 in the serum and the liver tissue of chronic HCV-infected patients. Arch Immunol Ther Exp 49:311, 2001.
23. Malaguarnera M, Di Fazio I, Romeo MA, Restuccia S, Laurino A, Trovato BA: Elevation of interleukin 6 levels in patients with chronic hepatitis due to hepatitis C virus. J Gastroenterol 32:211, 1997.
24. Frieling JT, van Hamersvelt HW, Wijdenes J, Hendriks T, Sauerwein RW, van Der Linden CJ: Circulating concentrations of soluble interleukin 6 receptors gp80 and gp130 in chronic renal failure and effects of renal replacement therapy. Am J Nephrol 19:571, 1999.
25. Dandona P, Aljada A, Bandyopadhyay A: Inflammation: the link between insulin resistance, obesity and diabetes. Trends Immunol 25:4, 2004.
26. Genesca J, Marti R, Gonzalez A, Torregrosa M, Segura R: Soluble interleukin-6 receptor levels in liver cirrhosis. Am J Gastroenterol 94:3074, 1999.
27. Rose-John S. Interleukin-6 biology is coordinated by membrane bound and soluble receptors. Acta Biochim Pol 50:603, 2003.
28. Montero-Julian FA: The soluble IL-6 receptors: serum levels and biological function. Cell Mol Biol 47:583, 2001.
29. Cressman DE, Greenbaum LE, DeAngelis RA, Ciliberto G, Furth EE, Poli V, Taub R: Liver failure and defective hepatocyte regeneration in interleukin-6-deficient mice. Science 274:1379, 1996.
30. Maione D, Di Carlo E, Li W, Musiani P, Modesti A, Peters M, Rose-John S, Della Rocca C, Tripodi M, Lazzaro D, Taub R, Savino R, Ciliberto G: Coexpression of IL-6 and soluble IL-6R causes nodular regenerative hyperplasia and adenomas of the liver. EMBO J 17:5588, 1998.
31. Schirmacher P, Peters M, Ciliberto G, Blessing M, Lotz J, Meyer zum Buschenfelde KH, Rose-John S: Hepatocellular hyperplasia, plasmacytoma formation, and extramedullary hematopoiesis in interleukin (IL)-6/soluble IL-6 receptor double-transgenic mice. Am J Pathol 153:639, 1998.

Combination Therapy of Intraarterial 5-Fluorouracil and Systemic Interferon-Alpha for Advanced Hepatocellular Carcinoma with Portal Venous Invasion

Shuntaro Obi, M.D.[1]
Haruhiko Yoshida, M.D.[2]
Risa Toune, M.D.[1]
Tadao Unuma, M.D.[1]
Miho Kanda, M.D.[2]
Shinpei Sato, M.D.[2]
Ryosuke Tateishi, M.D.[2]
Takuma Teratani, M.D.[2]
Shuichiro Shiina, M.D.[2]
Masao Omata, M.D.[2]

[1] Department of Hepatology, Kyoundo Hospital, Tokyo, Japan

[2] Department of Gastroenterology, Tokyo University, School of Medicine, Tokyo, Japan

BACKGROUND. Hepatocellular carcinoma (HCC) with portal venous invasion (PVI) has a very poor prognosis, with a median survival of 3 months and virtually no survival at 1 year. The combination of intraarterial 5-fluorouracil (FU) and systemic interferon-α (IFNα) was recently reported to be effective against HCC with PVI, but these were small pilot studies.

METHODS. One hundred and sixteen patients with HCC with PVI received IFNα (5,000,000 U intramuscularly on Days 1, 3, and 5 of each week of treatment) and 5-FU (500 mg into hepatic artery on Days 1-5 of the first and second week of each 4-week cycle). The therapy was either terminated at the end of the first cycle in cases with progressive disease, or continued for at least 3 cycles, when responses to treatment were evaluated by Eastern Cooperative Oncology Group criteria. The survival rate was compared with that of historical controls (n = 40).

RESULTS. Nineteen (16%) patients showed complete response and another 42 (36%) showed partial response. Adverse events were limited to nausea and appetite loss. The survival rates at 12 and 24 months among overall patients were 34% and 18%, respectively, in contrast to 15% and 5% among the historical controls. Survival rates at 12 and 24 months were 81% and 59% among complete responders, respectively, and 43% and 18% among partial responders.

CONCLUSION. The combination therapy with 5-FU and IFN was safe, and substantially improved the survival rate among the complete responders. These results provide a rationale for future randomized controlled trials. ***Cancer* 2006;106: 1990–7.** © *2006 American Cancer Society.*

KEYWORDS: carcinoma, hepatocellular, portal vein, drug therapy, interferons, fluorouracil.

Hepatocellular carcinoma (HCC) is one of the most common cancers worldwide, causing approximately 250,000 annual deaths.[1,2] The incidence of HCC has been increasing in Japan in the last 30 years[3] and also in the US more recently.[4] Advances in imaging techniques have facilitated the detection of HCC at early stages,[5–9] and those in therapeutic modalities, such as hepatic resection, percutaneous ethanol injection, radiofrequency ablation, and transplantation, have substantially improved the prognosis of HCC patients.[10–14] However, the long-term prognosis of HCC remains far from satisfactory, mainly because of the frequent recurrence of HCC.[15,16]

In particular, portal venous invasion (PVI), which is reported to develop in 16% to 65% of HCC cases,[17–20] is a common and serious sequela. First, tumor cells may spread out through the portal tract, resulting in extensive intrahepatic metastases. Second, portal vein occlusion may further deteriorate liver function, causing liver fail-

Address for reprints: Shuntaro Obi, M.D., Department of Hepatology, Kyoundo Hospital, 1-8 Kandasurugadai, Chiyoda, Tokyo 101-0062, Japan; Fax: (011) 81-3-3292-3376; E-mail: obishun@imail.plala.or.jp

Received 29 June 2005; revision received 28 September 2005; accepted 9 November 2005.

DOI 10.1002/cncr.21832
Published online 24 March 2006 in Wiley InterScience (www.interscience.wiley.com).

ure. Third, portal hypertension may be aggravated and lead to intractable ascites or variceal rupture.[21–26] These sequelae are often lethal by themselves, and will contraindicate further treatment of HCC, including liver transplantation.

Surgical resection of PVI has been reported but the results were disappointing.[27–29] Transcatheter chemoembolization to necrotize PVI have also been reported to necrotize PVI, but the results were unsatisfactory.[30,31] Arterial or systematic infusion of chemotherapeutic agents are rarely effective.[32–35] Radiation is sometimes effective against PVI, but the indication is often limited by the extent of the lesion or impaired liver function.[36]

The combination of interferon-α (IFNα) and 5-fluorouracil (5-FU) was first reported by Wadler et al.[37] in 1989 using advanced colorectal cancer. In 1993, Patt et al.[38] reported the effectiveness of combination of intramuscular IFNα and intravenous 5-FU in HCC patients. Subsequently, Urabe et al.[39] reported the combination of IFNα, 5-FU, cisplatin, methotrexate, and folinic acid in 1998. In 2002, Sakon et al.[40] reported the efficacy and safety of the combination of systemic IFNα and 5-FU administered to the hepatic artery in 8 HCC patients with PVI. Encouraged by these preliminary reports, we started to treat HCC patients with PVI with the combination therapy. In this study, we report the results of 116 consecutive HCC patients with PVI treated with the combination of IFNα and 5-FU, and compared the outcomes of 40 patients who were previously treated otherwise.

MATERIALS AND METHODS

Patients

HCC and PVI were diagnosed with contrast-enhanced computed tomography (CT) or magnetic resonance imaging. The staging of PVI was also aided by Doppler ultrasonography. Ultrasound-guided tumor biopsy was also performed when differentiation from nontumorous portal thrombosis was required. Eligibility criteria were as follows: HCC with PVI to at least 1 of the main branches of the portal vein; no indication for radiation therapy; an Eastern Cooperative Oncology Group (ECOG) performance status[41] of 0-2 (bed rest less than 50% of the daytime or better); no uncontrollable ascites; leukocyte count $>$ 3000/μL; platelet count $>$ 50,000/μL; total bilirubin $<$ 3.0 mg/dL; serum creatinine $<$ 1.5 mg/dL, and no contraindication for the implantation of the intraarterial catheter and the drug delivery system. During the study, we amended the criteria to exclude patients with extrahepatic metastases. We chose 40 other HCC patients with PVI we had treated previously with other modalities than the combination therapy as historical controls. They received radiation therapy (n = 8), intraarterial chemotherapy with epirubicin hydrochloride (n = 6), or supportive care only (n = 26) between August 1994 and August 2000.

Response Assessment

Before treatment, patients were evaluated by physical examination including the evaluation of performance status, laboratory tests including tumor markers, and CT, which was performed within 4 weeks before the commencement of therapy.

CT was repeated at the end of each therapeutic cycle to assess the response to treatment. The response was classified according to the ECOG criteria as: complete response when all measurable lesions disappeared including signs, symptoms, and biochemical changes related to the tumor, which must have lasted for more than 4 weeks, and no appearance of new lesions; partial response when the sum of the products of the greatest perpendicular dimension of each lesion was reduced by more than 50% and no appearance of new lesions; stable disease when the reduction was smaller than 50% or there was a smaller than 25% increase and no appearance of new lesions; and progressive disease when the increase was greater than 25% or appearance of new lesions.

Implantation of Arterial Catheter

An indwelling intraarterial catheter (Anthron P-U Catheter, TORAY, Tokyo, Japan) was inserted by direct femoral arterial puncture and its tip was put in the proper or common hepatic artery, embolizing the right gastric and the gastroduodenal arteries to avoid efflux of chemotherapeutic agents into the stomach and duodenum. The other end of the catheter was connected to a drug delivery system (P-U Celsite Port, TORAY) subcutaneously implanted in the lower abdomen.

Treatment Protocol

Patients who provided fully informed written consent were treated according to the protocol below. One cycle of treatment consisted of 4 weeks, where 5,000,000 U (5 MU) IFNα (OIF; Otsuka Pharmaceutical, Tokyo, Japan) was administered intramuscularly on Days 1, 3, and 5 of each week, resulting in a total dose of 60 MU in a cycle. 5-FU (500 mg/day, Kyowa Hakko, Tokyo, Japan) was administered into the hepatic artery over 5 hours using a portable infusion

TABLE 1
Baseline Clinical Characteristics

Characteristics*	IFN + 5-FU	Control	P
No. of patients	116	40	
Age, y§	62.7 ± 9.1	64.5 ± 8.4	.29†
Gender male/female	95/21	32/8	.79‡
Extent of portal vein invasion: trunk/first branch	28/88	15/25	.23‡
Tumor location: unilobular/bilobular	28/88	15/22	.10‡
Tumor size (cm)§	9.3 ± 3.8	8.4 ± 4.0	.09†
Child-Pugh status: A/B/C	7/89/10	6/29/5	.14‡
Total bilirubin (mg/dL)§	1.2 ± 0.9	1.4 ± 1.0	.35†
Albumin (g/dL)§	3.4 ± 0.5	3.3 ± 0.5	.24†
AST (IU/L)§	99.7 ± 63.4	86.7 ± 29.4	.21†
ALT (IU/L)§	64.5 ± 77.5	65.6 ± 17.3	.93†
Prothromin time (%)§	81.5 ± 14.1	79.3 ± 13.1	.38†
Platelet count ($\times 10^9$/L)§	143,000 ± 82,000	116000 ± 65000	.06†
α-fetoprotein (Positivity (≥ 20 ng/mL) %, median ng/mL)‖	83%, 969	95%, 546	.84†
Des-γ-carboxy prothrombin (Positivity (≥ 40 AU/mL)%, median AU/mL)‖	86%, 1585.0	87%, 1307.0	.06†
Etiology : HBV/HCV/HBV + HCV/others	23/77/1/15	7/31/0/2	.44†

AST: aspartate aminotransferase; ALT: alanine aminotransferase; HBV: hepatitis B virus; HCV: hepatitis C virus.
* The demographics of the 2 study groups. Control group was not significantly different from IFN + 5-FU group.
† Student *t*-test.
‡ Fisher exact test.
§ Mean ± SD.
‖ Data are expressed as numbers (%).

pump on Days 1-5 of the first and second weeks through the intraarterial catheter (5 g in a cycle).

At the end of each cycle the response to the therapy was assessed as described above. The combination therapy was discontinued in patients with progressive disease; otherwise, the treatment was repeated for at least 2 more cycles. The therapy was terminated in the event of a level 3 adverse effect according to the ECOG classification. Exceptions were changes in platelet count, leukocyte count, and total bilirubin that were attributable to cirrhosis and fever that was attributable to IFN.

Statistical Analyses

The difference of mean was analyzed with Student *t*-test. The difference in frequency distribution was analyzed with Fisher exact test or the chi-square test. Predisposing factors for the complete response to the combination therapy, as evaluated by the above criteria, were analyzed with logistic regression, where each continuous variable was transformed into a binary variable divided by the median value. In survival time analysis, data collection ended on December 10, 2004. Cumulative survival was calculated using the Kaplan-Meier method and the difference among the groups was analyzed with the log rank test. Independent factors for survival were assessed with the Cox proportional hazard regression model, including the comparison with historical controls. All statistic calculations were performed with SAS v. 8 (Cary, NC).

RESULTS

Patient Profile

A total of 116 patients, 95 men and 21 women, with an average age of 64 years (range, 39-79) received the combination therapy between September 2000 and May 2004 (Table 1). The etiology of the background liver disease was hepatitis C virus (HCV) in 78 patients, hepatitis B virus (HBV) in 24 (one positive also for HCV), and non-B non-C hepatitis in 15. Eighty-eight patients had PVI at a major branch (Vp 3) and 28 in the main trunk (Vp 4). The mean size of intrahepatic HCC tumor was 8 cm in diameter (range, 2-15). The baseline characteristics of 40 historical controls are also shown in the Table 1. There were no differences in tumor characteristics or liver function between the 2 groups.

All of the patients received at least 1 cycle of the combination therapy (range, 1-7 cycles; average, 2.1 cycles). The combination therapy was discontinued when the response was revealed to be progressive disease. Otherwise, the treatment was repeated, up to 4 or 5 times, so far as general conditions permitted. All of the 116 patients received the combination therapy: 1 cycle: 48 (41%) patients, 2 cycles: 32 (28%)

TABLE 2
Univariate Analysis of Predictors for Complete Response

Variables*†	Odds Ratio	95% CI	P
Age (> 64 y)	1.021	0.965–1.079	.4729
Gender (male)	0.797	0.235–2.702	.7155
Portal vein invasion (main trunk)	0.811	0.245–2.681	.7314
Platelet count (>120,000 $\times 10^9$/L)	0.943	0.871–1.022	.1541
Total bilirubin (>1.0 mg/dl)	0.892	0.496–1.602	.7014
Albumin (> 3.3 g/dL)	0.662	0.239–1.837	.4283
AST (> 85 IU/L)	1.003	0.996–1.010	.3538
ALT (> 51 IU/L)	1.000	0.993–1.007	.9370
Prothrombin time (> 81%)	0.966	0.930–1.003	.0736
α-fetoprotein (> 970 ng/mL)	0.742	0.275–2.006	.5570
Des-γ-carboxy prothrombin (> 1585 AU/mL)	0.848	0.316–2.275	.7440
HCV antibody (positive)	5.242	1.145–24.002	.0328‡

AST: aspartate aminotransferase; ALT: alanine aminotransferase; HCV: hepatitis C virus; CI: confidence interval.
* Univariate analysis of clinical, biochemical, and pathologic risk factors for complete response.
† The median value of each parameter is indicated in parentheses.
‡ Statistical significance.

TABLE 3
Multivariate Analysis of Predictors for Complete Response

Variables*†	Odds Ratio	95% CI	P
Platelet count (> 120,000 $\times 10^9$/L)	0.961	0.878–1.052	.3875
Prothrombin time (> 81%)	0.984	0.943–1.026	.4499
HCV antibody (positive)	4.262	0.896–20.267	.0683

HCV: hepatitis C virus; CI: confidence interval.
* Multivariate logistic regression analysis of complete response. Those factors with $P < .2$ in the univariate analysis (Table 2) were included.
† The median value of each parameter is indicated in parentheses.

patients, 3 cycles: 20 (17%) patients, 4 cycles or more: 16 (14%) patients.

Response to Treatment

Nineteen (16.4%) patients had a "complete response," 42 (36.2%) had "partial response," 2 (1.7%) had "stable disease," and 53 (45.7%) "progressive disease," resulting in a response rate (complete and partial responses) of 52.6%. The average duration of complete and partial responses was 13.6 and 4.8 months, respectively. The complete response rate was higher among patients with HCV infection (22%) than among others (5%) (Tables 2, 3). The final response to treatment was predictable, with the early response of tumor biomarker levels at Week 2 among patients whose markers were positive before treatment (α-fetoprotein (AFP) was positive (> 20 ng/mL) in 88%; L3 fraction of AFP (>15%) in 73%; and des-γ-carboxy prothrombin (DCP) (> 40 AU) in 87%, and at least 1 marker was positive in 97%). Patients with decreased tumor marker levels at Week 2 were very likely to achieve a final partial or complete response (90% sensitivity and 80% specificity).

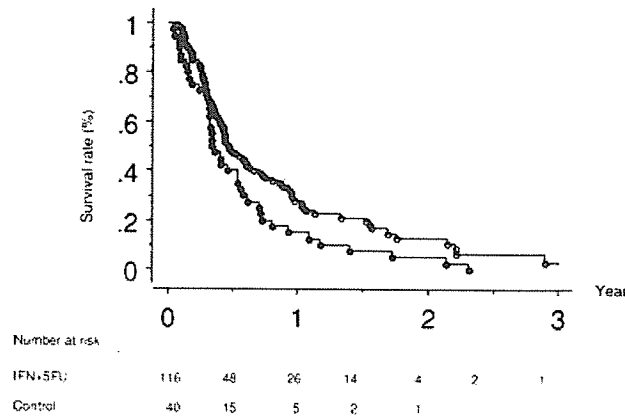

FIGURE 1. Comparison of the overall survival rate across the IFN + 5FU and control groups. The rate was significantly higher in the IFN + 5FU groups than in the control group ($P < .01$). Open circle, IFN + 5FU group; open triangle, control group.

Safety

Fever occurred in about 90% of patients, usually after the first IFN administration and gradually improved during subsequent administrations. An elevated aspartate aminotransferase (AST) level and decreased leukocyte or platelet count were found in 60% to 80% of patients, but none resulted in termination of the therapy or required granulocyte-colony-stimulating factor (G-CSF) administration. Nausea and vomiting, mostly ECOG Grade 1, occurred in about 50% patients. There was 1 case of stomatitis and another of depression (Grade 3 adverse event). The latter patient was the only case of discontinuation of treatment during the first cycle. There were no complications resulting from the arterial catheter.

Survival

Cumulative survival among all patients treated with the combination therapy is shown in Figure 1. The survival rates at 6, 12, and 24 months were 53%, 34%, and 18%, respectively, with a median survival of 6.9 months, compared with a survival rate of 40%, 15%, and 5%, respectively, in the historical control group. The survival was significantly different between the 2 groups ($P < .01$ by the log-rank test).

As shown in Figure 2, the response to treatment significantly affected survival. The complete responders showed the best survival rate of 81% and 59% at 12 and 24 months, respectively. In contrast, patients with

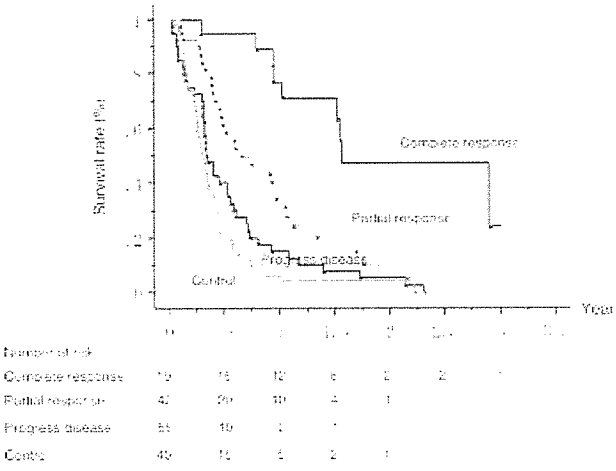

FIGURE 2. Comparison of the overall survival rate across the complete response, partial response, progress disease, and control groups. The rate was significantly higher in the complete response group than in the other 3 groups. Open circle, complete response group; open triangle, partial response group; open square, progressive disease group; closed circle, control group.

TABLE 4
Univariate Analysis of Predictors for Survival

Variables[*†]	Risk Ratio	95% CI	*P*
Age (>64 y)	0.999	0.977–1.021	.9344
Gender (male)	0.898	0.516–1.565	.7054
Portal vein invasion (main trunk)	0.503	0.302–0.837	.0081[‡]
Platelet count (>120,000 x10^9/L)	1.006	0.981–1.031	.6373
Total bilirubin (<1.0 mg/dl)	1.481	1.210–1.813	.0001[‡]
Albumin (>3.3 g/dL)	0.694	0.445–1.083	.1078
AST (>85 IU/L)	1.002	1.000–1.005	.0832
ALT (>51 IU/L)	1.003	1.000–1.005	.0329[‡]
Prothrombin time (>81%)	1.000	0.987–1.014	.9941
α-fetoprotein (>970 ng/mL)	0.948	0.626–1.434	.8012
Des-γ-carboxy prothrombin (>1585 AU/mL)	0.672	0.441–1.024	.0645
HCV antibody (positive)	1.357	0.867–2.124	.1812
Complete response	5.457	2.603–11.442	<.0001[‡]

AST: aspartate aminotransferase; ALT: alanine aminotransferase; HCV: hepatitis C virus; CI: confidence interval.

[*] Univariate analysis of clinical, biochemical, and pathologic risk factors for survival.

[†] The median value of each parameter is indicated in parentheses.

[‡] Statistical significance.

stable disease or progressive disease had poorer outcomes, comparable to the historical control. Patients with a partial response showed an intermediate prognosis, with a survival rate of 43% and 18% at 12 and 24 months, respectively. Univariate (Table 4) and multivariate analyses (Table 5) showed that the predictors for survival were complete response ($P<.0001$), cycle number ($P = .0038$), VP grade ($P = .0123$), and total bilirubin concentration ($P = .0339$). HCC invasion into the main trunk of the portal vein and total bilirubin concentration greater than 1.0 mg/dL predicted a poor prognosis independent of the treatment response.

TABLE 5
Multivariate Analysis of Predictors for Survival

Variables[*†]	Risk ratio	95% CI	*P*
Portal vein invasion (main trunk)	0.0043	1.041–1.938	.0043[‡]
Total bilirubin (<1.0 mg/dl)	1.420	1.041–1.938	.0267[‡]
Albumin (>3.3 g/dL)	0.669	0.357–1.192	.1742
AST (>85 IU/L)	1.002	0.997–1.006	.2692
ALT (>51 IU/L)	1.000	0.995–1.004	.8807
Des-γ-carboxy prothrombin (>1585 AU/mL)	1.000	1.000–1.000	.1166
HCV antibody (positive)	1.191	0.722–1.963	.4939
Complete response	7.293	3.359–15.837	<.0001[‡]

AST: aspartate aminotransferase; ALT: alanine aminotransferase; HCV: hepatitis C virus; CI: confidence interval.

[*] Stepwise multiple Cox regression analysis in the IFN + 5-FU group. Those variables with $P<.2$ in univariate analysis (Table 4) were included.

[†] The median value of each parameter is indicated in parentheses.

[‡] Statistical significance.

Case Presentation

A 63-year-old male underwent a partial hepatectomy for HCC in March 1998. One year after surgery, multiple intrahepatic recurrences were found and transcatheter arterial embolization (TAE) was performed. Despite repeated TAE, recurrences continued to occur. Massive HCC in segment 4 and PVI for the right main portal branch appeared in August 2002. The patient received the combination therapy (3 cycles) between September 2002 and November 2002, which resulted in a decrease in the DCP level from 14,400 to 30 and also in the AFP level from 96,497 to 48. At the end of therapy, a CT scan showed no evidence of HCC with PVI and the portal blood flow was recovered (Fig. 3).

DISCUSSION

In the present study, the combination chemotherapy with IFNα and 5-FU showed an objective response rate of 52% among HCC patients with PVI. In particular, 16% of patients achieved a complete response, namely disappearance of PVI and intrahepatic HCC nodules that lasted at least 4 weeks. The improvement in survival rate was remarkable among those patients, showing a survival rate of 81% and 59% at 1 and 2 years, respectively. These figures were in distinct contrast to the 15% and 5% among the historical controls. In the previous report by Sakon et al.,[40] the combination therapy of 5-FU and IFNα demonstrated better responses than ours. The discrepancy may be due to

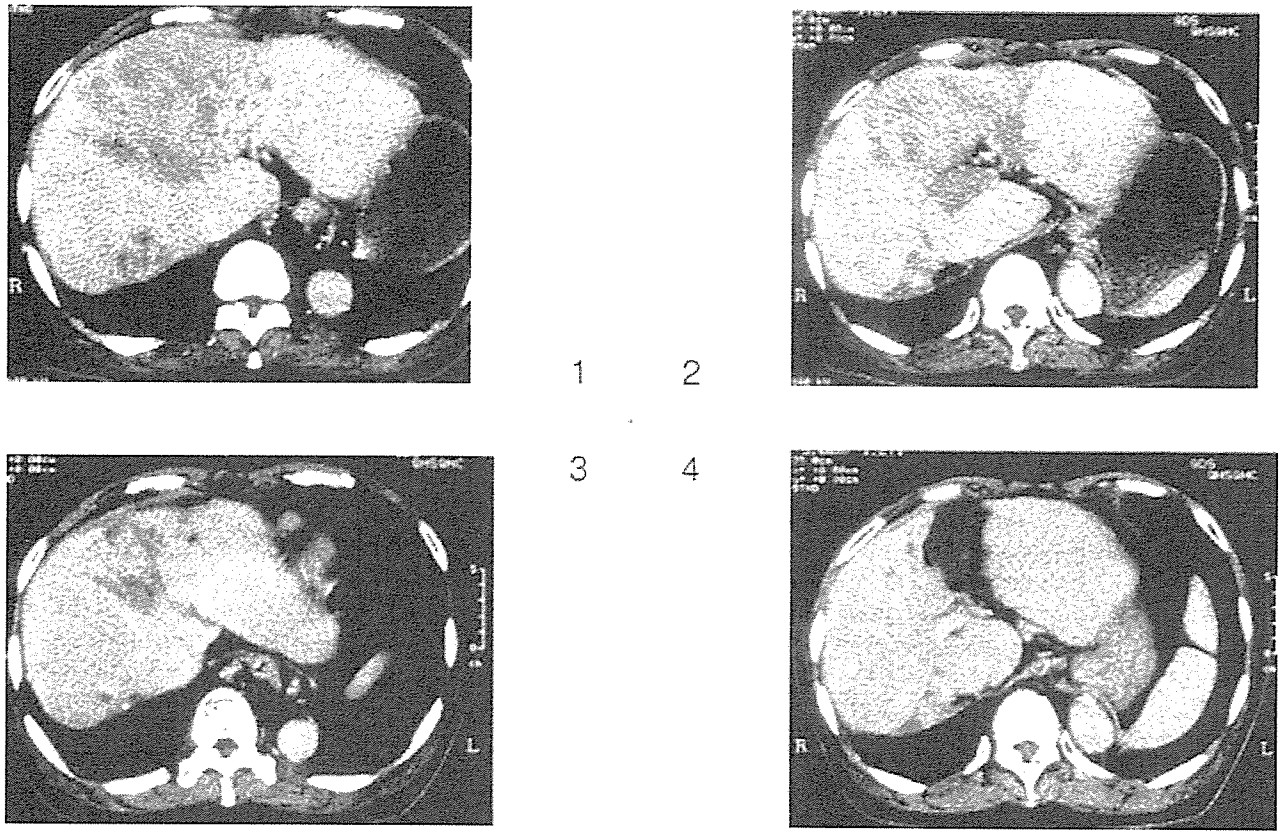

FIGURE 3. Abdominal CT scan before the combination therapy. Massive HCC existed in segments 4 and 8 (1), with invasion into the right main branch of portal vein blocking portal blood flow (2). Abdominal computed tomography scan after the combination therapy. Massive HCC disappeared (3) and the portal blood flow reappeared (4).

the following. First, the current study included HCC patients with invasion not only into a major branch but also into the main trunk (28%). Second, the majority of patients in this study were recurrent cases (74%). Third, total bilirubin level was greater than 1.0 mg/dL in the majority of patients (67%), indicating poorer liver function and prognosis.

Reports using monotherapy with intraarterial 5-FU showed lower response rates, ranging from 13% to 22%, with a median survival of only 3.5 to 14 months.[33–35] Monotherapy with IFNα, once thought to be an omnipotent anticancer drug, hardly demonstrated clinical effects against HCC.[42] Thus, the combination of the 2 agents seems to have some synergism, but the mechanism of action is not known yet. It was recently reported that IFNα induces p53, which enhances apoptotic responses to 5-FU.[43] We examined the combination of IFNα and 5-FU in 8 distinct human HCC lines and found that IFNα markedly increases susceptibility to 5-FU in 5 of the 8 cells.[44] Several genes showed distinct gene expression profiles in the responsive cells and others. Further investigation of these genes may elucidate underlying molecular mechanisms, enabling us to predict the efficacy of this combination therapy.

Despite the prominent improvement in survival among complete responders, we must admit that the complete response rate, 16%, was not satisfactory. Although it may be possible to enhance the response among partial responders by modifying the protocol, we suspect that about half of the patients with HCC will remain unsusceptible to the combination therapy and we cannot predict responders beforehand. Fortunately, adverse events were rarely severe and all were manageable in this study. At present, we recommend starting the combination therapy with close monitoring of response, preferably that of tumor biomarkers, and treatment should be continued if there is a response after the first cycle of chemotherapy.

We found in the early phase of this study that the combination of IFNα and intraarterial 5-FU is not effective against extrahepatic metastases. This is understandable because 5-FU, administered into the hepatic artery, will not reach extrahepatic tissues in high

concentrations. However, systemic administration of 5-FU or related agents may be effective against extrahepatic lesions in combination with IFNα. This possibility is highly interesting because the implantation of an indwelling catheter is one of the demerits of the present combination therapy. If the agent can be given in a less invasive way, we may be able to enlarge the indication so as to include less advanced HCC patients.

In conclusion, we show that the combination of systemic IFNα and intraarterial 5-FU is effective in a subset of HCC patients with PVI, which resulted in disappearance of PVI and intrahepatic HCC nodules in 16% of patients. These complete responders showed survival rates of 81% and 59% at 12 and 24 months, respectively.

REFERENCES

1. Shiratori Y, Yoshida H, Omata M. Management of hepatocellular carcinoma: advances in diagnosis, treatment and prevention. *Anticancer Ther.* 2001;1:277–290.
2. Boring CC, Squires TS, Tong T. Cancer statistics. *CA Cancer J Clin.* 1992;42:19–38.
3. Okuda K, Fujimoto I, Hanai A, Urano Y. Changing incidence of hepatocellular carcinoma in Japan. *Cancer Res.* 1987;47: 4967–4972.
4. El-Serag HB, Mason AC. Rising incidence of hepatocellular carcinoma in the United States. *N Engl J Med.* 1999;340:745–750.
5. Shinagawa T, Ohto M, Kimura K, et al. Diagnosis and clinical features of small hepatocellular carcinoma with emphasis on the utility of real-time ultrasonography: a study in 51 patients. *Gastroenterology.* 1984;2:S21–26.
6. Takayasu K, Moriyama N, Muramatsu Y, et al. Hepatic arterial embolization for hepatocellular carcinoma. Comparison of CT scans and resected specimens. *Radiology.* 1984; 150:661–665.
7. Yoshida H, Itai Y, Ohtomo K, Kokubo T, Minami M, Yashiro N. Small hepatocellular carcinoma and cavenous hemangioma: differentiation with dynamic FLASH MR imaging with Gd-DTPA. *Radiology.* 1989;171:339–342.
8. Takayasu K, Shima Y, Muramatsu Y, et al. Angiography of small hepatocellular carcinomas: analysis of 105 resected tumors. *Am J Roentgenol.* 1986;147:525–529.
9. Matsui O, Takashima T, Kadoya M, et al. Dynamic computed tomography during arterial portography; the most sensitive examination for hepatocellular carcinomas. *J Comput Assist Tomogr.* 1985;9:19–24.
10. Makuuchi M, Hasegawa H, Yamazaki S. Ultrasonically guided subsegmentectomy. *Surg Gynecol Obestet.* 1985;161: 346–350.
11. Ohtomo K, Furui S, Kokubo T, et al. Transcatheter arterial embolization (TAE) in treatment for hepatoma—analysis of three-year survivors. *Radiat Med.* 1985;3:176–180.
12. Shiina S, Tagawa K, Niwa Y, et al. Percutaneous ethanol injection therapy for hepatocellular carcinoma: result in 146 patients. *Am J Roentogenol.* 1993;160:1023–1028.
13. Shiina S, Teratani T, Obi S, et al. Non surgical treatment of hepatocellular carcinoma: from percutaneous ethanol injection therapy and percutaneous microwave coagulation therapy to radiofrequency ablation. *Oncology.* 2002;62(Suppl 1): 64–68.
14. Roayaie S, Frischer JS, Emre SH, et al. Long-term results with multimodal adjuvant therapy and liver transplantation for the treatment of hepatocellular carcinoma larger than 5 centimeters. *Ann Surg.* 2002;235:533–539.
15. Lin TY, Lee CS, Chen KM, et al. Role of surgery in the treatment of primary carcinoma of the liver: a 31-year experience. *Br J Surg.* 1987;74:839–842.
16. Koike Y, Shiratori Y, Sato, et al. Risk factors for recurring hepatocellular carcinoma differ according to infected hepatitis virus—an analysis of 236 consecutive patients with a single lesion. *Hepatology.* 2000;32:1216–1223.
17. Albacete RA, Matthews MJ, Nirmal S. Portal vein thromboses in malignant hepatoma. *Ann Intern Med.* 1967;67:337–347.
18. Tobe T, Takayasu K, Kasugai F, et al. The Liver Cancer Study Group of Japan. Primary liver cancer in Japan. Clinicopathologic features and results of surgical treatment. *Ann Surg.* 1990;211:277–287.
19. Adachi E, Maeda T, Kajiyama K, et al. Factors correlated with portal venous invasion by hepatocellular carcinoma. Univariate and multivariate analysis of 232 resected cases without preoperative treatments. *Cancer.* 1996;77:2022–2031.
20. Toyosaka A, Okamoto E, Mitsunobu M, Oriyama T, Nakao N, Miura K. Intra hepatic metastasis in hepatocellular carcinoma: evidence for spread via the portal vein as an efferent vessel. *Am J Roentogenol.* 1996;91:1610–1615.
21. The Liver Cancer Study Group of Japan. Predictive factors for long term prognosis after partial hepatectomy for patient with hepatocellular carcinoma in Japan. *Cancer.* 1997;74: 2772–2780.
22. Cady B. Natural history of primary and secondary tumors of the liver. *Semin Oncol.* 1983;10:127–134. Review.
23. Yamanaka N, Okamoto E, Toyosaka A, et al. Prognostic factors after hepatectomy for hepatocellular carcinomas. A univariate and multivariate analysis. *Cancer.* 1990;65:1104–1110.
24. Fuster J, Garcia-Valdecasas JC, Grande L, et al. Hepatocellular carcinoma and cirrhosis. Results of surgical treatment in European series. *Ann Surg.* 1996;223:297–302.
25. Johnson RC. Hepatocellular carcinoma. *Hepatogastroenterology.* 1997;44:307–312.
26. Hsu HC, Wu TT, Wu MZ, Sheu JC, Lee CS, Chen DS. Tumor invasiveness and prognosis in HCC. *Cancer.* 1988;61:2095–2099.
27. Asahara T, Itamoto T, Katayama K, et al. Hepatic resection with tumor thrombectomy for hepatocellular carcinoma with tumor thrombi in the major vasculature. *Hepatogastroenterology.* 1999;46:1862–1869.
28. Tanaka A, Morimoto T, Yamaoka Y. Implications of surgical treatment for advanced hepatocellular carcinoma with tumor thrombi in the portal vein. *Hepatogastroenterology.* 1996;43:637–643.
29. Yamaoka Y, Kumada K, Ino K, et al. Liver resection for hepatocellular carcinoma with direct removal of tumor thrombi in the main portal vein. *World J Surg.* 1992;16:1172–1176.
30. Furuse J, Iwasaki M, Yoshino M, et al. Hepatocellular carcinoma with portal vein tumor thrombus: embolization of arterioportal shunt. *Radiology.* 1997;204:787–790.

31. Yen FS, Wu JC, Kuo BI, Chiang JH, Chen TZ, Lee SD. Transcatheter arterial embolization for hepatocellular carcinoma with portal vein thrombosis. *J Gastroenterol Hepatol.* 1995; 10:237–240.
32. Ando E, Yamashita F, Tanaka M, Tanikawa K. A novel chemotherapy for advanced hepatocellular carcinoma with tumor thrombosis of the main trunk of the portal vein. *Cancer.* 1997;79:1890–1896.
33. Stehlin JS Jr., de Ipolyi PD, Greeff PJ, McGaff CJ Jr., Davis BR, McNary L. Treatment of cancer of the liver: twenty years experience with infusion and resection in 414 patients. *Ann Surg.* 1988;208:23–25.
34. Doci R, Bignami P, Bozzetti F, et al. Intrahepatic chemotherapy for unresectable hepatocellular carcinoma. *Cancer.* 1988;61:1983–1987.
35. Iwamiya T, Sawada S, Ohta Y. Repeated arterial infusion chemotherapy for inoperable hepatocellular carcinoma using an implantable drug delivery system. *Cancer Chemother Pharmacol.* 1994;33:S134–138.
36. Chen SC, Lian SL, Chang WY. The effect of external radiotherapy in treatment of portal vein invasion in hepatocellular carcinoma. *Cancer Chemother Pharmacol.* 1994;33:124–127.
37. Wadler S, Schwartz EL, Goldman M, et al. Fluorouracil and recombinant alfa-2a-interferon: an active regimen against advanced colorectal carcinoma. *J Clin Oncol.* 1989;7:1769–1775.
38. Patt YZ, Yoffe B, Charnsangavej C, et al. Low serum alpha-fetoprotein level in patients with hepatocellular carcinoma as a predictor of response to 5-FU and interferon-alpha-2b. *Cancer.* 1993;72:2574–2582.
39. Urabe T, Kaneko S, Matsushita E, Unoura M, Kobayashi K. Clinical pilot study of intrahepatic arterial chemotherapy with methotrexate, 5-fluorourasil, cisplatin, and subcutaneous interferon-alpha-2b for patients with locally advanced hepatocellular carcinoma. *Oncology.* 1998;55:39–47.
40. Sakon M, Nagano H, Dono K, et al. Combined intraarterial 5-fluorouracil and subcutaneous interferon-alpha therapy for advanced hepatocellular carcinoma with tumor thrombi in the major portal branches. *Cancer.* 2002;94:435–442.
41. Oken MM, Creech RH, Tormey DC, et al. Toxicity and response criteria of the Eastern Cooperative Oncology Group. *Am J Clin Oncol.* 1982;5:649–655.
42. Llovet JM, Sala M, Castells L, et al. Randomized controlled trial of interferon treatment for advanced hepatocellular carcinoma. *Hepatology.* 2000;31:54–58.
43. Takaoka A, Hayakawa S, Yanai H, et al. Integration of interferon-alpha/beta signally to P53 responses in tumor suppression and antiviral defense. *Nature.* 2003;424:516–523.
44. Moriyama M, Hoshida Y, Kato N, et al. Genes associated with human hepatocellular carcinoma cell chemosensitivity to 5-fluorouracil plus interferon-alpha combination chemotherapy. *Int J Oncol.* 2004;25:1279–1287.

Oncogene (2006) 25, 633–642

www.nature.com/onc

ORIGINAL ARTICLE

The hepatitis B virus X protein enhances AP-1 activation through interaction with Jab1

Y Tanaka[1], F Kanai[1,2], T Ichimura[3], K Tateishi[1], Y Asaoka[1], B Guleng[1], A Jazag[1], M Ohta[1], J Imamura[1], T Ikenoue[1], H Ijichi[1], T Kawabe[1], T Isobe[3] and M Omata[1,2]

[1]Department of Gastroenterology, Graduate School of Medicine, University of Tokyo, Tokyo, Japan; [2]Clinical Research Center, University of Tokyo Hospital, Tokyo, Japan and [3]Department of Chemistry, Graduate School of Science, Tokyo Metropolitan University, Hachioji-shi, Tokyo, Japan

Hepatitis B virus X protein (HBx) has many cellular functions and is a major factor in hepatitis and hepatocellular carcinoma caused by HBV infection. A proteomic approach was used to search for HBx-interacting proteins in order to elucidate the molecular mechanism of hepatocarcinogenesis. HBx was attached to myc and flag tags (MEF tags) and expressed in 293T cells; the protein complex formed within the cells was purified and characterized by mass spectrometry. COP9 signalosome (CSN) subunits 3 and 4 were subsequently identified as HBx-interacting proteins. In addition, CSN subunit 5, Jun activation domain-binding protein 1 (Jab1), was shown to be a novel cellular target of HBx. *In vivo* and *in vitro* interactions between HBx and Jab1 were confirmed by standard immunoprecipitation and GST pull-down assays. An analysis of HBx deletion constructs showed that amino acids 30–125 of HBx were responsible for binding to Jab1. Confocal laser microscopy demonstrated that HBx was mainly localized in the cytoplasm, while Jab1 was found mainly in the nucleus and partially in the cytoplasm, and that the two proteins colocalized in the cytoplasm. The cotransfection of HBx and Jab1 resulted in substantial activator protein 1 (AP-1) activation and knockdown of endogenous Jab1 attenuated AP-1 activation caused by HBx. In addition, the coexpression of HBx and Jab1 potentiated phosphorylation of JNK, leading to the subsequent phosphorylation of c-Jun, whereas the level of c-Jun and JNK phosphorylation induced by HBx was decreased in Jab1 knockdown cells. These results suggest that the interaction between HBx and Jab1 enhances HBx-mediated AP-1 activation.
Oncogene (2006) **25,** 633–642. doi:10.1038/sj.onc.1209093; published online 10 October 2005

Keywords: HBV; HBx; AP-1; Jab1; HCC

Correspondence: Dr F Kanai, Department of Gastroenterology, Graduate School of Medicine, University of Tokyo, 7-3-1 Hongo, Bunkyo-ku, Tokyo 113-8655, Japan.
E-mail: kanaif-int@h.u-tokyo.ac.jp
Received 9 May 2005; revised 27 July 2005; accepted 3 August 2005; published online 10 October 2005

Introduction

Persistent hepatitis B virus (HBV) infection is closely associated with the development of the acute and chronic forms of hepatitis, and with cirrhosis and hepatocellular carcinoma (HCC) (Ganem and Varmus, 1987). Although worldwide more than 300 million people are chronically infected, the exact molecular mechanism of HBV pathology remains uncertain and an effective treatment for the eradication of HBV has not been found (Omata, 1998). HBV, a member of the hepadnavirus family, has a partially double-stranded, circular DNA genome consisting of four open reading frames (ORFs) that encode viral proteins. One such ORF, the X gene, encodes the 154-amino-acid HBV X protein (HBx), which has been assigned a variety of cellular functions, including viral infection (Zoulim *et al.*, 1994), viral replication (Bouchard *et al.*, 2001), and signal transduction. Moreover, the expression of HBx induces the transformation of murine fibroblasts and causes the development of hepatocellular carcinoma in certain strains of transgenic mice (Shirakata *et al.*, 1989; Kim *et al.*, 1991), albeit the link between HBx and hepatocarcinogenesis is still controversial.

A number of studies have shown that HBx acts as a transcriptional *trans*-activator of several cellular and viral genes, including proto-oncogenes, suggesting a mechanism of HCC development. HBx has also been reported to interact with DNA-binding proteins involved in transcriptional regulation, including the TATA-binding protein (Qadri *et al.*, 1995), the RPB5 subunit (Cheong *et al.*, 1995), and the cAMP-response-element-binding protein/transcription-activating protein (CREB/ATF) (Maguire *et al.*, 1991), and to act as a coactivator of transcription. HBx was also shown to stimulate transcription indirectly by activating cellular signal-transduction pathways, and several transcription elements activated by HBx have been identified, for example, the Ras-Raf-mitogen-activated protein kinase (MAPK) cascade (Benn and Schneider, 1994; Natoli *et al.*, 1994), that are essential for activator protein 1 (AP-1) activation. The AP-1 transcription factor is a dimeric complex of the Jun (c-Jun, JunB, and JunD), Fos (c-Fos, FosB, Fra1, and Fra2), activating

transcription factor (ATF), and musculoaponeurotic fibrosarcoma (Maf) protein families, which recognize either TPA response elements (TRE) or the cAMP response element (CRE).

AP-1 activation is induced by a variety of physical and chemical stresses, including cytokines, growth factors, and bacterial and viral infections. Such stimuli activate the MAP kinase cascade, leading to the activation of MKK4 and MKK7, and the subsequent phosphorylation of c-Jun amino-terminal kinase (JNK) in the cytoplasm. Following these events, JNK translocates to the nucleus and phosphorylates the activation domain of c-Jun at serine residues 63 and 73, leading to the enhancement of its transcriptional activity. AP-1 exerts its oncogenic effects by regulating genes involved in cell proliferation, differentiation, apoptosis, angiogenesis, and tumor invasion (Shaulian and Karin, 2002; Eferl and Wagner, 2003). The constitutive activation of the MAPK signaling pathway is involved in many types of cancers, including HCC (Ito *et al.*, 1998), and the precise mechanism of the activation of this pathway by HBx has been explored intensively. HBx activates proline-rich tyrosine kinase-2 (Pyk2) via calcium signaling (Bouchard *et al.*, 2001) and the downstream Src family kinase (Klein and Schneider, 1997; Klein *et al.*, 1999), leading to subsequent Ras-Raf activation (Benn and Schneider, 1994). Also, HBx has been shown to trigger the N-terminal phosphorylation of c-Jun via activation of JNK, which stimulates the prolonged synthesis of c-Jun (Benn *et al.*, 1996). Other group has demonstrated that HBx causes the phosphorylation of c-Jun (Ser-63), resulting in AP-1 activation (Henkler *et al.*, 1998). Furthermore, the sustained activation of JNK and subsequent AP-1 activation was observed in mice transfected with HBx via a virus-mediated delivery system (Nijhara *et al.*, 2001b).

Although many studies have been reported, the precise mechanism of AP-1 activation by HBx is still not well defined. To investigate the molecular mechanism of hepatocarcinogenesis caused by HBx, we employed a novel tandem affinity purification (MEF) method (Ichimura *et al.*, 2005) and mass spectrometry (MS), which allowed us to identify the COP9 signalosome (CSN) subunits 3 and 4 as novel HBx-binding proteins. CSN was first identified in *Arabidopsis thaliana* as an eight-subunit complex involved in the suppression of light-dependent development (Wei and Deng, 1999). Using the yeast two-hybrid system, the fifth CSN subunit, Jun activation domain-binding protein 1 (Jab1), was identified as a binding protein of the activation domain of c-Jun (Claret *et al.*, 1996), whereby it acts as a coactivator of c-Jun and JunD in the stabilization of the AP-1 complex with its binding sites, thus increasing the specificity of the target-gene activation.

In this study, we demonstrate that HBx directly interacts with Jab1 and that this interaction results in substantial AP-1 activation. The elucidation of this interaction will aid in clarifying the mechanism of hepatocyte proliferation and hepatocarcinogenesis.

Results

Identification of CSN subunits 3 and 4 as HBx-interacting proteins by mass spectrometry

To search for HBx-interacting proteins, a novel tandem affinity purification (MEF) method was employed (Ichimura *et al.*, 2005). This technique uses two different affinity modules (myc and flag) separated by a cleavage site for the TEV protease (myc-TEV-flag). A mammalian expression vector encoding HBx with an amino-terminal MEF tag was constructed and used to transiently transfect 293T cells. Tagged HBx with its binding proteins was then purified from the cell lysate. After the proteins were eluted with flag peptides, they were separated by SDS–PAGE and silver stained. Figure 1 shows the SDS–PAGE profiles

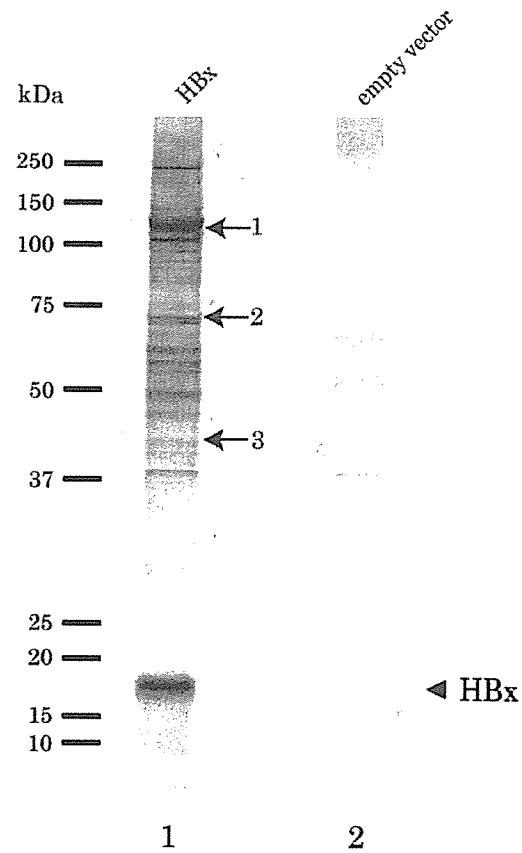

Figure 1 Affinity-purified proteins that bind to HBx. 293T cells transfected with pcDNA3-MEF-HBx or pcDNA3-MEF were lysed, and the expressed HBx was recovered using the MEF procedure. The proteins bound to HBx were eluted from the beads, separated by SDS–PAGE (10/20%), and silver stained. Lane 1, pcDNA3-MEF-HBx; lane 2, pcDNA3-MEF. The molecular masses of the protein standards are indicated. The arrowhead indicates the position of HBx. The 12 protein bands were excised from the gel and subjected to in-gel tryptic digestion. The positions of UV-damaged DNA-binding protein 1 (DDB1) (band 1), heat-shock protein 70 (band 2), and COP9 signalosome (CSN) subunits 3 and 4 (band 3) are indicated by the arrows.

Table 1 Identification of CSN subunits 3 and 4 by tandem mass spectrometry

Protein	*Accession number (GI)*	*Peptide m/z*	*Charge*	*Sequence determined*	*Residues*
CSN subunit 3	23238222	616.5418	2+	YILVSLILLGK	227–237
		742.0447	2+	TFLTLSLQDMASR	313–325
		874.6328	2+	AMDQEITVNPQFVQK	392–406
CSN subunit 4	6753490	689.5337	2+	VISFEEQVASIR	96–107
		819.6502	2+	NAAQVLVGIPLETGQK	122–137
		641.5153	2+	AVIEHNLLSASK	303–314
		1110.347	2+	LYNNITFEELGALLEIPAAK	315–334
		553.4229	2+	IASQMITEGR	338–347

of the dissociated proteins. The bands in lane 1 (cells transfected with pcDNA3-MEF-HBx) are proteins that directly or indirectly bound to HBx, whereas no proteins were detected in lane 2 (cells transfected with pcDNA3-MEF). The 12 major protein bands were excised from the gel and subjected to in-gel tryptic digestion. The resultant peptides were extracted from the gel slice and analysed using the direct nano-flow LC-MS/MS system, which identified 10 proteins. Among them we detected known targets of HBx, UV-damaged DNA-binding protein 1 (DDB1) (Figure 1, band 1) (Sitterlin *et al*., 1997), and heat–shock protein 70 (Figure 1, band 2) (Zhang *et al*., 2005), and these interactions were confirmed by immunoprecipitation followed by immnoblot (data not shown). Table 1 describes the identified peptide sequences of the 40 kDa band (Figure 1, band 3). The most significant hits for this band were obtained with CSN subunits 3 and 4, and this band contained two proteins which had similar molecular weight.

HBx interacts with Jab1 in vivo *and* in vitro

The protein identified by mass spectrometry, CSN, is composed of eight subunits. The CSN complex contains Jab1, a coactivator of c-Jun that activates AP-1 (Claret *et al*., 1996). The proteins found on the gel were not Jab1 but had previously been shown to be associated with Jab1 in the CSN complex. As HBx expression also induces AP-1 activation (Benn *et al*., 1996), a role for Jab1 in HBx-mediated AP-1 activation was examined by studying the interaction between these two proteins. To investigate whether HBx binds to endogenous Jab1 in a cellular context, HBx was introduced into 293T cells, and immunoprecipitation with anti-flag antibody was performed. As shown in Figure 2a, immunoprecipitation followed by immunoblotting demonstrated that HBx interacted with Jab1 in 293T cells. To examine whether HBx binds to Jab1 *in vitro*, GST-HBx and GST were incubated with *in vitro*-translated Jab1, and a pull-down assay was performed. Figure 2b shows that GST-HBx bound to Jab1 *in vitro*. These results demonstrated that HBx directly interacts with Jab1. The interaction between HBx and Jab1 seems much more efficient in total cell lysates than with protein transcribed and translated *in vitro*, which suggests that other factors are necessary to stabilize the interaction.

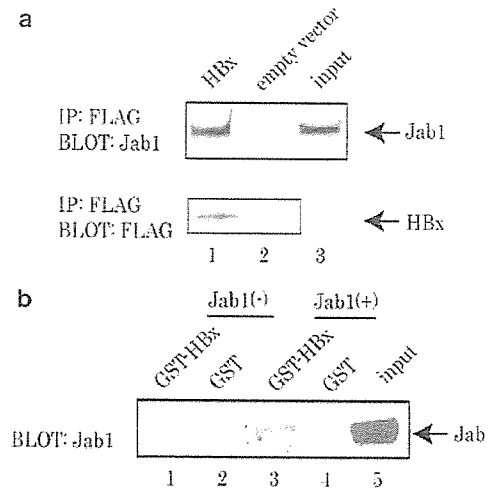

Figure 2 Interaction of HBx and Jab1 *in vivo* and *vitro*. (**a**) 293T cells were transfected with the following plasmids: lane 1, pcDNA3-MEF-HBx, 2 μg; lane 2, pcDNA3-MEF, 2 μg; lane 3, input (1/20 of the cell extracts). After 48 h, the cells were harvested, and the lysates were immunoprecipitated with anti-flag antibody followed by immunoblotting with the corresponding antibodies. (**b**) GST-HBx and GST were incubated with *in vitro*-translated Jab1, and a pull-down assay was then performed. Lane 1, GST-HBx (control); lane 2, GST (control); lane 3, GST-HBx incubated with Jab1; lane 4, GST incubated with Jab1; lane 5, input (1/50 of the *in vitro*-translated Jab1). Bound Jab1 was probed with streptavidin conjugated with HRP.

Amino acids 30–125 of HBx are necessary for binding to Jab1

To further characterize the HBx-binding site involved in the interaction with Jab1, immunoprecipitation was carried out using the following deletion mutants of HBx: HBx (1–125), HBx (1–105), HBx (30–154), and HBx (61–154) (Figure 3a). All of the constructs except HBx (1–105) and HBx (61–154) bound endogenous Jab1 (Figure 3b). This result was confirmed by carrying out the same experiment using the construct HBx (30–125), followed by immunoprecipitation. Although the interaction was weak, this construct also bound Jab1, indicating that amino acids 30–125 of HBx are necessary for binding to Jab1. It should be noted that the region containing amino acids 30–125 includes part of the *trans*-activation function of HBx (Murakami *et al*., 1994).

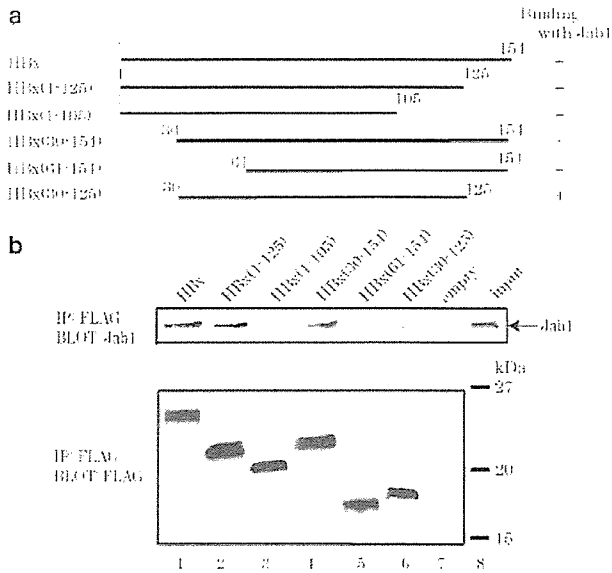

Figure 3 Mapping of the Jab1-interacting region of HBx. (**a**) Schematic presentation of the HBx and HBx deletion mutants that were analysed. The binding of HBx with Jab1 is shown in the right panel. (**b**) 293T cells were transfected with the following plasmids: lane 1, pcDNA3-MEF-HBx, 2 μg; lane 2, pcDNA3-MEF-HBx (1 125), 2 μg; lane 3, pcDNA3-MEF-HBx (1–105), 2 μg; lane 4, pcDNA3-MEF-HBx (30–154), 2 μg; lane 5, pcDNA3-MEFHBx (61–154), 2 μg; and lane 6, pcDNA3-MEF-HBx (30–125), 2 μg; lane 7, pcDNA3-MEF, 2 μg; and lane 8, input (1/20 of the cell extracts). Cell lysates were immunoprecipitated with anti-flag antibody followed by immunoblotting with the corresponding antibodies. The molecular masses of the protein standards are indicated.

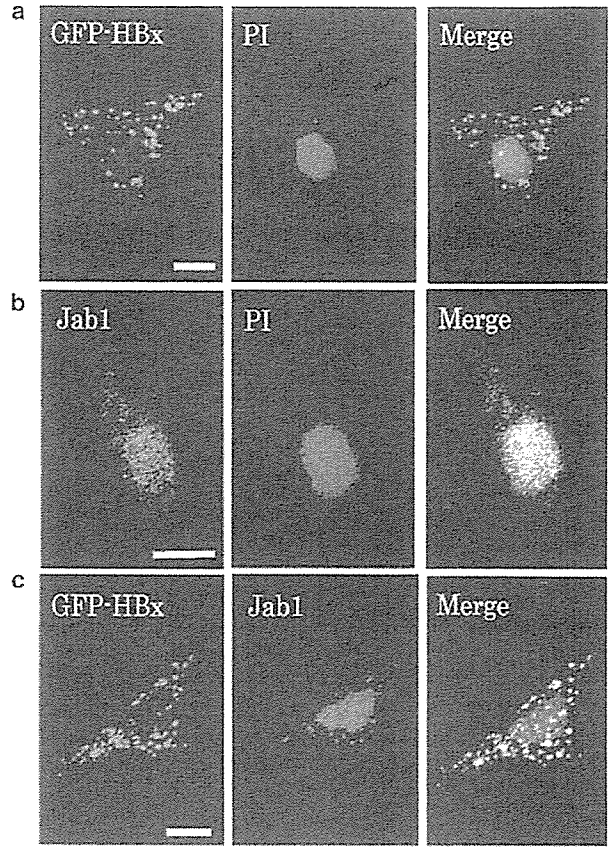

Figure 4 Subcellular localization of HBx and Jab1 in HeLa cells (**a**) Localization of transfected GFP-HBx (green). HeLa cells were transfected with pEGFP-X; after 24 h, the nuclei were stained with propidium iodide (red). (**b**) Localization of endogenous Jab1 (green). HeLa cells were immunostained with anti-Jab1 antibody and secondary antibody Alexa Fluor 488 (green), and the nuclei were stained with propidium iodide. (**c**) Localization of GFP-HBx (green) and endogenous Jab1 (red). The cells were transfected with pEGFP-X; after 24 h, endogenous Jab1 was immunostained with anti-Jab1 antibody and Alexa 555 goat anti-mouse IgG secondary antibody. Merged images are shown in the right panel. Bar = 10 μm.

HBx and Jab1 colocalize in the cytoplasm

To assess the subcellular localization of HBx and Jab1, cells were examined by immunocytochemistry using confocal microscopy. pEGFP-X, the GFP-tagged HBx expression vector, was transfected into HeLa cells, and the nuclei were stained with propidium iodide. As reported previously, HBx was mainly localized in the cytoplasm rather than in the nucleus (Henkler *et al*., 2001) (Figure 4a), whereas endogenous Jab1 was mainly localized in the nucleus and partially in the cytoplasm (Figure 4b). We also investigated the localization of flag-tagged HBx, which had a similar distribution to GFP-tagged HBx (data not shown), and was consistent with a previous report (Doria *et al*., 1995). As shown in Figure 4c, the expression of HBx did not affect the main localization of Jab1, although Jab1 in the cytoplasm seems to cluster in the presence of HBx. While a small amount of Jab1 was localized in the cytoplasm, it mostly colocalized with HBx (Figure 4c). These results suggest that small but significant part of Jab1 and HBx colocalized in the cytoplasm.

Jab1 facilitates HBx-mediated AP-1 activation

To investigate the effect of Jab1 on HBx-mediated AP-1 activation, HeLa cells were cotransfected with HBx and Jab1 expression plasmids and then assayed for luciferase activity. Biochemical assay revealed that only small amount of overexpressed Jab1 was incorporated into the CSN complex (Naumann *et al*., 1999). The introduction of Jab1 alone did not induce significant AP-1 activation (2.0$\pm$0.4 times) (Figure 5a, lane 2), nor did HBx alone (2.4$\pm$0.6 times) (Figure 5a, lane 3). However, the cotransfection of HBx and Jab1 increased reporter activity to a level 8.2$\pm$1.3 times that of the control (Figure 5a, lane 4) ($P<0.05$). These data suggest that Jab1, not CSN complex, is involved in HBx-mediated AP-1 activation. To further investigate the role of endogenous Jab1 for AP-1 activation by HBx, we established Jab1 knockdown HeLa cell lines using the stable RNAi and performed luciferase assay. Figure 5b shows the establishment of the Jab1 knockdown (JAB1KD) HeLa cells. Wild-type HeLa cells or JAB1KD HeLa cells were cotransfected with HBx and AP-1 reporter plasmids and then assayed for luciferase activity. As shown in Figure 5c, HBx activated AP-1 in a

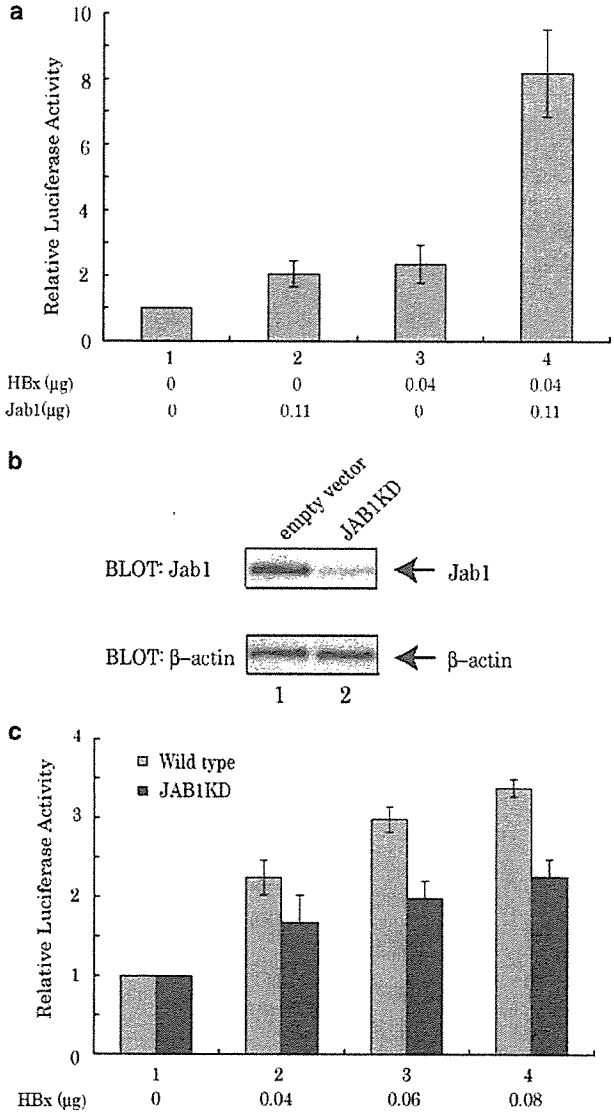

Figure 5 Jab1 facilitates HBx-mediated AP-1 activation. (**a**) The effects of HBx and Jab1 on AP-1 activation. HeLa cells were transfected with 0.14 μg pAP-1-Luc and 0.01 μg pRL-TK plus: lane 1, pCMV, 0.15 μg; lane 2, pcDNA3-flag-Jab1, 0.11 μg, and pCMV, 0.04 μg; lane 3, pEF-BOS-HBx, 0.04 μg, and pCMV, 0.11 μg; lane 4, pEF-BOS-HBx, 0.04 μg, and pcDNA3-flag-Jab1, 0.11 μg. After 24 h, the cells were harvested and subjected to a luciferase assay. Luciferase activity was normalized by taking the activity of the empty vector as 1 (relative luciferase activity). The results represent the mean (bar) ± s.d. (line) of at least three independent experiments. (**b**) Confirmation of Jab1 knockdown (JAB1KD) HeLa cells. HeLa cells were transfected with pcPUR + U6icassette or pcPUR + U6-Jab1i and incubated with puromycin to select stably transfected cells. They were harvested, and the lysates were immunoblotted with the corresponding antibodies: lane 1, wild-type HeLa cell pool; lane 2, JAB1KD HeLa cell pool. (**c**) Dose-dependent activation of the AP-1 promoter with HBx in wild-type and JAB1KD HeLa cells. The cells were transfected with 0.14 μg pAP-1-Luc and 0.01 μg pRL-TK plus: lane 1, pCMV, 0.15 μg; lane 2, pEF-BOS-HBx, 0.04 μg, and pCMV, 0.11 μg; lane 3, pEF-BOS-HBx, 0.06 μg, and pCMV, 0.09 μg; or lane 4, pEF-BOS-HBx, 0.08 μg, and pCMV, 0.07 μg. Luciferase activity was normalized by taking the activity of the empty vector as 1 (relative luciferase activity). The results represent the mean (bar) ± s.d. (line) of at least three independent experiments.

dose-dependent manner, which is consistent with a previous report (Kato *et al*., 2000). However, the AP-1 activation in JAB1KD HeLa cells is attenuated (2.3 ± 0.2 times) compared with wild-type HeLa cells (3.4 ± 0.1 times) ($P < 0.05$). These results suggest that endogenous Jab1 is partially involved in HBx-mediated AP-1 activation.

Coexpression of HBx and Jab1 potentiates JNK and c-Jun phosphorylation

AP-1 activation is induced in part by the phosphorylation of c-Jun (Shaulian and Karin, 2002; Eferl and Wagner, 2003). To further investigate the mechanism of AP-1 activation by HBx and Jab1, the phosphorylation status of c-Jun was examined. HeLa cells were cotransfected with the HA-tagged c-Jun, HBx, and Jab1 expression vectors. After 24 h, the cells were harvested, proteins were immunoprecipitated with anti-HA antibody, and the level of c-Jun phosphorylation was examined using a phospho-specific antibody. As previously shown, Jab1 or HBx caused the phosphorylation of c-Jun (Figure 6a, lanes 2 and 3) (Henkler *et al*., 1998; Kleemann *et al*., 2000). In addition, the cotransfection of HBx and Jab1 modestly, but reproducibly, enhanced the phospho-c-Jun level compared with the transfection of HBx or Jab1 only (Figure 6a, lane 4). The phosphorylation level of JNK, an upstream molecule that activates c-Jun, was also investigated.

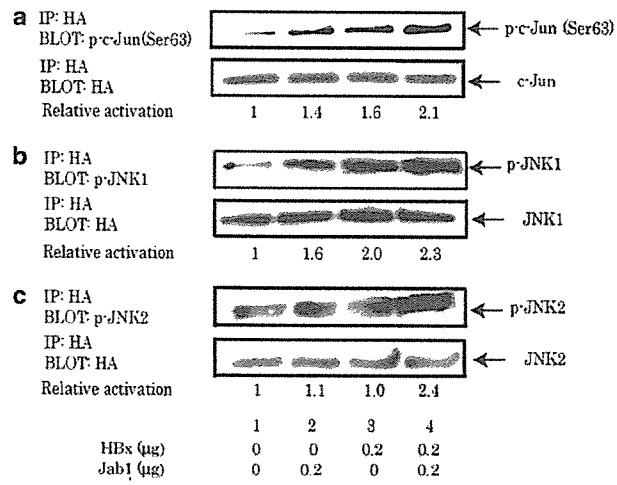

Figure 6 Jab1 enhances HBx-induced phosphorylation of c-Jun and JNK. HeLa cells in a 6 cm dish were transfected with 0.6 μg HA-tagged c-Jun (**a**), JNK1 (**b**), or JNK2 (**c**) expression vector and the following combination of plasmids; lane 1, pCMV, 0.4 μg; lane 2, pcDNA3-flag-Jab1, 0.2 μg, and pCMV, 0.2 μg; lane 3, pEF-BOS-HBx, 0.2 μg, and pCMV, 0.2 μg; lane 4, pEF-BOS-HBx, 0.2 μg, and pcDNA3-flag-Jab1, 0.2 μg. After 24 h, the cells were harvested, and HA-tagged c-Jun or JNK was immunoprecipitated with anti-HA antibody. The status of c-Jun and JNK phosphorylation was probed with anti-phospho-c-Jun (Ser-63) antibody and anti-phospho-SAPK/JNK (Thr-183/Tyr-185) antibody, respectively. The total amount of immunoprecipitated c-Jun and JNK was probed with anti-HA antibody. Quantification of relative activation was also indicated. Representative experiments among at least three independent experiments are shown.

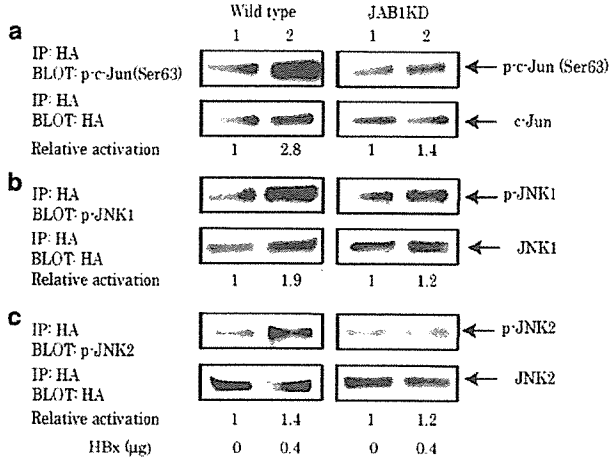

Figure 7 Phosphorylation of c-Jun and JNK induced by HBx is attenuated in Jab1 knockdown (JAB1KD) HeLa cells. Wild-type or JAB1KD HeLa cells in a 6-cm dish were transfected with 0.6 μg HA-tagged c-Jun (**a**), JNK1 (**b**), or JNK2 (**c**) expression vector and the following combination of plasmids; lane 1, pEF-BOS, 0.4 μg; lane 2, pEF-BOS-HBx, 0.4 μg. After 24 h, the cells were harvested, and HA-tagged c-Jun or JNK was immunoprecipitated with anti-HA antibody. The status of c-Jun and JNK phosphorylation was probed with anti-phospho-c-Jun (Ser-63) antibody and anti-phospho-SAPK/JNK (Thr-183/Tyr-185) antibody, respectively. The total amount of immunoprecipitated c-Jun and JNK was probed with anti-HA antibody. Quantification of relative activation was also indicated. Representative experiments among at least three independent experiments are shown.

Both JNK1 and JNK2 phosphorylation were higher in cells coexpressing HBx and Jab1 than in cells expressing HBx or Jab1 only (Figure 6b and c). To further examine the effect of endogenous Jab1 on the phosphorylation of c-Jun and JNK induced by HBx, wild-type or JAB1KD HeLa cells were transfected with HBx and the level of c-Jun and JNK phosphorylation was investigated. As shown in Figure 7, the phosphorylation of c-Jun (Figure 7a) and JNK1 (Figure 7b) was attenuated in JAB1KD HeLa cells compared with wild-type HeLa cells. There was no significant change in JNK2 phosphorylation between wild-type and JAB1KD HeLa cells (Figure 7c), probably because JNK2 phosphorylation induced by HBx was modest (Figures 6c and 7c). These results suggest that Jab1 binds to HBx and that this interaction potentiates the phosphorylation of JNK and c-Jun, leading to AP-1 activation.

Discussion

In the present study, a novel MEF method applied in combination with nano-flow LC-MS/MS analysis was used to show that CSN subunits 3 and 4 interact with HBx. CSN subunit 5, Jab1, was not directly identified by this technique but assumed present based on the presence of other CSN subunits. The direct binding of HBx with Jab1 and the importance of amino acids 30–125 of HBx in the association with Jab1 were also demonstrated. Furthermore, our results suggest that small but significant fraction of HBx and Jab1 interact in the cytoplasm and that this interaction enhances the phosphorylation of JNK and c-Jun, with subsequent AP-1 activation.

The tandem affinity purification method was originally developed to analyse interactions among yeast proteins (Rigaut *et al.*, 1999). We constructed a mammalian expression vector with two different tags, myc and flag, containing a TEV protease cleavage site (Ichimura *et al.*, 2005). This technique results in highly purified proteins and a low background. This method enabled us to identify 10 HBx-interacting proteins, and the interactions between HBx and other identified proteins are under investigation. The dual-tag method followed by MS analysis can be used to identify novel protein–protein interactions in mammalian cells.

CSN is composed of eight subunits and is involved in protein phosphorylation (Bech-Otschir *et al.*, 2001; Uhle *et al.*, 2003), protein degradation (Tomoda *et al.*, 1999), and deneddylation (Cope *et al.*, 2002) in mammalian cells. Each subunit has been identified as the binding partner of many other proteins and thus has specific functions (Bech-Otschir *et al.*, 2002). We analysed only 12 major protein bands by MS analysis; however other CSN subunits including Jab1 were not identified.

Several groups have reported that the subcellular distribution of HBx is predominantly cytosolic and that a small amount of HBx is localized in the nucleus (Doria *et al.*, 1995; Henkler *et al.*, 2001). Endogenous Jab1 is mainly incorporated into the CSN complex in the nucleus, but recent studies suggest that Jab1 is also found as a smaller form in the cytoplasm, where it consists of only a subset of CSN components (Oron *et al.*, 2002; Tomoda *et al.*, 2002). It has also been reported that cytoplasmic, but not nuclear, HBx activates the Ras-Raf-MAPK cascade, leading to AP-1 activation (Doria *et al.*, 1995). These results support our data on the interaction between HBx and Jab1 in the cytoplasm and subsequent AP-1 activation. Although the main localization of the two molecules differs, immunocytochemistry suggests that HBx interacts with Jab1 *in vivo*.

We have shown that the induction of HBx and Jab1 causes AP-1 activation. HBx activates AP-1 via two distinct pathways, the Ras-Raf-MAPK and the JNK cascades. HBx stimulates both JNKs and ERKs, leading to the induction and activation of the AP-1 promoter (Benn *et al.*, 1996). Jab1 was first identified as a coactivator of c-Jun (Claret *et al.*, 1996), and the expression of Jab1 leads to significant AP-1 activity. However, some groups reported that the overexpression of Jab1 did not greatly affect AP-1 activation (Naumann *et al.*, 1999). Furthermore, the mechanism of c-Jun activation by Jab1 is still unknown. In the nucleus, Jab1 stabilizes c-Jun together with its promoter region and activates specific gene transcription (Claret *et al.*, 1996). In the cytoplasm, Jab1 activates JNK and enhances the endogenous phospho-c-Jun level (Kleemann *et al.*, 2000). However, some groups reported that c-Jun activation caused by CSN is independent of JNK

(Naumann *et al.*, 1999). These conflicting results might be owing to the complexity of Jab1 interactions; for example, whether the function of Jab1 involves a CSN-independent or CSN-associated form has not been determined (Chamovitz and Segal, 2001).

In our study, the coexpression of HBx and Jab1 induced synergistic AP-1 activation to a greater extent than that obtained with HBx or Jab1 alone and knockdown of endogenous Jab1 attenuates AP-1 activation caused by HBx. While only a small portion of Jab1 might interact with HBx *in vivo*, cytoplasmic Jab1 could bind to HBx and potentiate its activity to phosphorylate JNK. Knockdown of endogenous Jab1 did not lead to complete suppression of AP-1 activation by HBx, thus another pathway such as Ras-Raf-MAPK cascade might be involved in the activation of AP-1. HBx mutant lacking the Jab1-interacting domain (HBx 61–154) still partially activates AP-1 promoter (data not shown), which is consistent with a previous report that HBx 58–140 can still activate AP-1 (Nijhara *et al.*, 2001a). These data also suggest the involvement of another signaling pathway in AP-1 activation. Whereas ectopically expressed Jab1 was also reported to be associated with protein ubiquitination and degradation, including that of p27 (Tomoda *et al.*, 1999), HIF 1α (Bae *et al.*, 2002), and TGFβ (Wan *et al.*, 2002), the coexpression of HBx and Jab1 did not result in these or similar functions (data not shown).

Recently, c-Jun was reported to play an important role in hepatocyte proliferation and apoptosis, and AP-1 was found to be activated in clinical samples of hepatocellular carcinoma and chronic hepatitis (Liu *et al.*, 2002). Furthermore, a liver-specific c-Jun knockout mouse model revealed that this protein is required in the early stages of tumor development, by preventing apoptosis induced by p53 activity (Eferl *et al.*, 2003). Taken together, these data suggest that the prolonged expression of HBx leads to sustained AP-1 activation and induces hepatocarcinogenesis.

In conclusion, we have demonstrated that Jab1 interacts with HBx and enhances HBx-mediated AP-1 activation. Our results contribute to elucidating the mechanisms of HBV-mediated hepatocarcinogenesis.

Materials and methods

Cell lines and transfection

The human embryonic kidney cell line 293T and the human cervical carcinoma cell line HeLa were purchased from the Riken Cell Bank (Tsukuba Science City, Japan) and were maintained in Dulbecco's modified Eagle's medium (Sigma, St Louis, MO, USA) containing 10% heat-inactivated fetal bovine serum. The cells were transfected using the Effectene transfection reagent (Qiagen, Hilden, Germany) according to the manufacturer's instructions.

Antibodies

Mouse monoclonal anti-c-myc (EQKLISEEDL) antibody (9E10) conjugated with agarose was obtained from Santa Cruz Biotechnology (Santa Cruz, CA, USA). Mouse monoclonal anti-flag M2 (DYKDDDDK) antibody and its agarose-conjugated form and mouse monoclonal anti-β-actin antibody were purchased from Sigma. The mouse monoclonal anti-HA (hemagglutinin: YPYDVPDYA) antibody (12CA5) was obtained from Roche Diagnostics (Indianapolis, IN, USA). Mouse monoclonal and rabbit polyclonal anti-Jab1 antibodies were from Genetex (San Antonio, TX, USA) and Santa Cruz Biotechnology, respectively. Rabbit polyclonal anti-phospho-c-Jun (Ser-63) II antibody and anti-phospho-SAPK/JNK (Thr-183/Tyr-185) antibody were purchased from Cell Signaling (Beverly, MA, USA). Alexa Fluor 488 goat anti-rabbit IgG secondary antibody and Alexa Fluor 555 goat anti-rabbit IgG secondary antibody were obtained from Molecular Probes (Eugene, OR, USA). Anti-mouse antibody, anti-rabbit antibody, and streptavidin-conjugated with horseradish peroxidase (HRP) were purchased from Amersham Biosciences (Uppsala, Sweden).

Plasmids

The mammalian expression plasmid for the MEF method, pcDNA3-MEF, was described previously (Ichimura *et al.*, 2005). Using pCXN2-HBx (Kato *et al.*, 2000) as a template, full-length HBx and its deletion fragments were amplified by PCR with the following sets of primers:

HBx 5′: CGGAATTCATGGCTGCTAGGCTGTG CTG,
HBx 3′: CCGCTCGAGTTAGGCAGAGGTGAA AAAGTT,
HBx (1–125) 5′: CGGAATTCATGGCTGCTAGGCTGTG CTG,
HBx (1–125) 3′: CGCTCGAGTTACTCCCCCAACTCCTC CCA,
HBx (1–105) 5′: CGGAATTCATGGCTGCTAGGCTGTG CTG,
HBx (1–105) 3′: CCGCTCGAGTTACGTTGACATTGCT GAGAG,
HBx (30–154) 5′: CGGAATTCTTCTCGGGGTCGCTTGG GACTC,
HBx (30–154) 3′: CCGCTCGAGTTAGGCAGAGGTGAA AAAGTT,
HBx (61–154) 5′: CGGAATTCTGTGCCTTCTCATCTGC CGG,
HBx (61–154) 3′: CCGCTCGAGTTAGGCAGAGGTGAA AAAGTT,
HBx (30–125) 5′: CGGAATTCTTCTCGGGGTCGCTTGG GACTC,

HBx (30–125) 3′: CGCTCGAGTTACTCCCCCAACTCCT CCCA. The PCR products were cloned into the *Eco*RI *and* *Xho*I sites of pcDNA3-MEF, producing pcDNA3-MEF-HBx, pcDNA3-MEF-HBx (1–125), pcDNA3-MEF-HBx (1–105), pcDNA3-MEF-HBx (30–154), pcDNA3-MEF-HBx (61–154), and pcDNA3-MEF-HBx (30–125), respectively.

The mammalian expression vector pEF-BOS, which is driven by the elongation factor-1α promoter, was previously described (Mizushima and Nagata, 1990). Using pCXN2-HBx as a template, full-length HBx was amplified by PCR with the following primers: HBx 5′: GCTCTAGAACCATGGCTG CTAGGCTGTGCT, HBx 3′: GCTCTAGATTAGGCAGAG GTGAAAAAGT. The PCR products were cloned into the *Xba*I site of pEF-BOS, producing pEF-BOS-HBx.

The flag-tagged Jab1 expression plasmid pcDNA3-flag-Jab1 was generously provided by David J Mann (Department of Biological Sciences, Imperial College of Science, Technology and Medicine, London, UK) (Chopra *et al.*, 2002). The EGFP-tagged HBx expression plasmid (pEGFP-X) was a gift from